

1

2 **On the annual variability of**

3 **Antarctic aerosol size**

4 **distributions at Halley research**

5 **station**

6

7 Thomas Lachlan-Cope¹, David Beddows², Neil Brough¹, Anna E.
8 Jones¹, Roy M. Harrison^{2,+}, Angelo Lupi³, Young Jun Yoon⁴, Aki
9 Virkkula^{5,6} and Manuel Dall’Osto^{7*}

10

11 ¹*British Antarctic Survey, NERC, High Cross, Madingley Rd, Cambridge, CB3*
12 *0ET, United Kingdom*

13 ²*National Center for Atmospheric Sciences, University of Birmingham,*
14 *Edgbaston, Birmingham, B15 2TT, United Kingdom*

15 ³*Institute of Atmospheric Sciences and Climate (ISAC), National Research*
16 *Council (CNR), via P. Gobetti 101, 40129, Bologna Italy*

17 ⁴*Korea Polar Research Institute, 26, SongdoMirae-ro, Yeonsu-Gu, Incheon,*
18 *KOREA 406-840*

19 ⁵*Institute for Atmospheric and Earth System Research, University of Helsinki*
20 *Helsinki, FI-00014, Finland*

21 ⁶*Finnish Meteorological Institute, FI-00101 Helsinki, Finland*

22 ⁷*Institute of Marine Sciences, Passeig Marítim de la Barceloneta, 37-49. E-*
23 *08003, Barcelona, Spain; corresponding author, email: dallosto@icm.csic.es*

24

25 ⁺Also at: Department of Environmental Sciences/Centre of Excellence in
26 Environmental Studies, King Abdulaziz University, PO Box 80203, Jeddah,
27 21589, Saudi Arabia.

1 **Abstract**

2

3 The Southern Ocean and Antarctic region currently best represent one of the
4 few places left on our planet with conditions similar to the preindustrial age.
5 Currently, climate models have low ability to simulate conditions forming the
6 aerosol baseline; a major uncertainty comes from the lack of understanding of
7 aerosol size distributions and their dynamics. Contrasting studies stress that
8 primary sea-salt aerosol can contribute significantly to the aerosol population,
9 challenging the concept of climate biogenic regulation by new particle
10 formation (NPF) from dimethyl sulphide marine emissions.

11 We present a statistical cluster analysis of the physical characteristics of
12 particle size distributions (PSD) collected at Halley (Antarctica) for the year
13 2015 (89% data coverage, 6-209 nm size range, daily size resolution). By
14 applying the Hartigan-Wong k-Means method we find 8 clusters describing the
15 entire aerosol population. Three clusters show *pristine* average low particle
16 number concentrations ($< 121\text{-}179\text{ cm}^{-3}$) with three main modes (30 nm, 75-
17 95 nm, 135-160 nm) and represent 57% of the annual PSD (up to 89-100%
18 during winter, 34-65% during summer based upon monthly averages).
19 Nucleation and Aitken mode PSD clusters dominate summer months (Sep-
20 Jan, 59-90%), whereas a clear bimodal distribution (43 and 134 nm,
21 respectively, Hoppel minimum at mode 75 nm) is seen only during the Dec-
22 Apr period (6-21%). Major findings of the current work include: (1) NPF and
23 growth events originate from both the sea ice marginal zone and the Antarctic
24 plateau, strongly suggesting multiple vertical origins, including marine
25 boundary layer and free troposphere; (2) very low particle number
26 concentrations are detected for a substantial part of the year (57%), including
27 summer (34-65%), suggesting that the strong annual aerosol concentration
28 cycle is driven by a short temporal interval of strong NPF events; (3) a unique
29 pristine aerosol cluster is seen with a bimodal size distribution (75 nm and 160
30 nm, respectively), strongly associated with high wind speed and possibly
31 associated with blowing snow and sea spray sea salt, dominating the winter
32 aerosol population (34-54%). A brief comparison with two other stations
33 (Dome C Concordia and King Sejong Station) during the year 2015 (240 days
34 overlap) shows that the dynamics of aerosol number concentrations and

1 distributions are more complex than the simple sulphate-sea spray binary
2 combination, and it is likely that an array of additional chemical components
3 and processes drive the aerosol population. A conceptual illustration is
4 proposed indicating the various atmospheric processes related to the
5 Antarctic aerosols, with particular emphasis on the origin of new particle
6 formation and growth.

7

8 **1 Introduction**

9

10 Atmospheric marine aerosol particles contribute substantially to the global
11 aerosol budget; they can impact the planetary albedo and climate (Reddington
12 et al., 2017). However, aerosols remain the least understood and constrained
13 aspect of the climate system (Boucher et al., 2013). Aerosol concentration,
14 size distribution, chemical composition and dynamic behavior in the
15 atmosphere play a crucial role in governing radiation transfer. However,
16 aerosol sources and processes, including critical climate feedback
17 mechanisms, are still not fully characterized. This is especially true in pristine
18 environments, where the largest uncertainties are found, mainly due to lack of
19 understanding of pristine natural sources (Carslaw et al., 2013). Indeed, the
20 Southern Ocean and the Antarctic region still raises many unanswered
21 atmospheric science questions. This region has complex interconnected
22 environmental systems - such as ocean circulation, sea ice, land and snow
23 cover – which are very sensitive to climate change (Chen et al., 2009).

24 Early research upon Antarctic aerosols was carried out over various part of
25 the continent and reviewed by Shaw et al. (1988). It was concluded that a
26 peculiar feature of the Antarctic aerosol system is a very pronounced annual
27 cycle of the total particle number concentration, with concentrations 20-100
28 times higher during austral summer than during winter.

29 This seasonal cycle - like a seasonal "pulse" over the summer months
30 (December, January and February) - seems to be more prominent in the
31 upper Antarctic plateau than the coastal Antarctic zones, but particle number
32 concentrations are much higher in coastal Antarctica. One possible origin for
33 these nuclei could be the Antarctic free troposphere, as suggested by Ito et al.

1 (1993), although this free troposphere to marine boundary layer transport was
2 considered by no means a definite explanation (Koponen et al., 2002; 2003).
3 Overall, the aerosol summer maximum concentrations can be largely
4 explained by new particle formation (NPF) events, as recently reviewed by
5 Kerminen et al., (2018).

6 The vertical origin of these NPF events is still matter of debate. Some
7 indications suggesting NPF takes place preferentially in the Antarctic Free
8 Troposphere (FT): aerosols originate in the upper troposphere, then the
9 circulation induced by the Antarctic drainage flow (James, 1989) transports
10 aerosols down to the boundary layer in the Antarctic plateau, with subsequent
11 transport further to the coast by katabatic winds (Ito et al., 1993; Koponen et
12 al., 2002; Fiebig et al., 2014; Hara et al., 2011; Järvinen et al., 2013;
13 Humphries et al., 2016). A recent study found that the Southern Ocean was
14 the dominant source region for particles observed at Princess Elisabeth (PE)
15 station, leading to an enhancement in particle number (N), while the Antarctic
16 continent itself was not acting as a particle source (Herenz et al., 2019).
17 Further studies also point to boundary layer oceanic sources of NPF events
18 (Weller et al., 2011; Weller et al., 2015; Weller et al., 2018). Recently, a long
19 term analysis of the seasonal variability in the physical characteristics of
20 aerosol particles sampled from the King Sejong Station (located on King
21 George Island at the top of the Antarctic Peninsula) was reported (Kim et al.,
22 2017). The CCN concentration during the NPF period increased by
23 approximately 11 % compared with the background concentration (Kim et al.,
24 2019). Interestingly, new particle formation events were more frequent in the
25 air masses that originated from the Bellingshausen Sea than in those that
26 originated from the Weddell Sea, and it was argued that the taxonomic
27 composition of phytoplankton could affect the formation of boundary layer new
28 particles in the Antarctic Ocean (Jang et al., 2019). Dall'Osto et al. (2017)
29 reported higher ultrafine particles in sea ice-influenced air masses.

30

31 Overall, studies to date suggest that regional NPF events in Antarctica are not
32 as frequent as those in the Arctic or other natural environments, although the
33 growth rates are similar (Kerminen et al., 2018). In terms of aerosol size, most
34 of the ultrafine (<100 nm) particle concentrations have been linked to NPF

1 events, whereas sea salt particles dominate the coarse mode and
2 accumulation mode (>100 nm). A recent study by Yang et al. (2019), however,
3 proposes a source for ultrafine sea salt aerosol particle from blowing snow,
4 dependent on snow salinity. This mechanism could account for the small
5 particles seen during Antarctic winter at coastal stations.

6
7 It is interesting to note that the recent, spatially-extensive study of the
8 concentration of sea-salt aerosol throughout most of the depth of the
9 troposphere and over a wide range of latitudes (Murphy et al., 2019) reported
10 a source of sea-salt aerosol over pack ice that is distinct from that over open
11 water, likely produced by blowing snow over sea ice (Huang et al., 2018;
12 Giordano et al., 2018; Frey et al., 2020). In recent years, a number of long
13 term aerosol size distribution datasets have been discussed (Järvinen et al.,
14 2013; Kim et al., 2019) but these types of datasets are still scarce. The ability
15 to measure aerosol size distributions at high time resolution allows open
16 questions to be investigated. The purpose of the present work is to examine
17 for the first time a one year long (2015) dataset collected at Halley Station.

18
19 Previous work at the Halley research station reported size-segregated aerosol
20 samples collected with a cascade impactor at 2 week intervals for a year. Sea
21 salt was found to be a major component of aerosol throughout the year (60%
22 of mass) deriving from the sea ice surface rather than open water.
23 Methanesulphonic Acid (MSA) and non-sea-salt sulphate both peaked in the
24 summer and were found predominantly in the submicron size range (Rankin
25 and Wolff, 2003). Observations of new particle formation during a two month
26 cruise in the Weddell Sea revealed an iodine source (Atkinson et al., 2012).
27 While no short-term correlation (timescale < 2 days) was found between
28 particles and iodine compounds in a later study (Roscoe et al., 2015), the
29 authors highlighted correlations on seasonal timescales. It is also worth
30 mentioning that a previous Weddell Sea study also found increased new
31 particle formation in the sea ice zone (Davison et al., 1996), but no clear
32 correlation between dimethyl sulphide and new particle bursts was found.

33

1 In this paper, we use k-means cluster analysis (Beddows et al., 2009) to
2 elucidate the properties of the aerosol size distributions collected across the
3 year 2015 at Halley. A clear advantage of this clustering method over
4 average size distributions (e.g. monthly, seasonally, etc.) is that specific
5 aerosol categories of PSD can be compared across different time periods, as
6 further described later in section 2. While a number of intensive polar field
7 studies have focused on average monthly datasets, cluster analyses of year
8 long polar and marine particle size distributions measurements are scarce. In
9 a nutshell, these clustering method can reduce the complexity of the PSD
10 dataset, allowing an smoother separation of different PSDs (Beddows et al.,
11 2014). Recently, cluster analysis was applied to Arctic aerosol size
12 distributions taken at Zeppelin Mountain Svalbard; Dall'Osto et al., 2017a)
13 during an 11-year record (2000–2010) and at Villum Research Station
14 (Greenland; Dall'Osto et al., 2018b) during a 5-year period (2012–2016). Both
15 studies showed a striking negative correlation between sea ice extent and
16 nucleation events, and concluded that NPF are events linked to biogenic
17 precursors released by open water and melting sea ice regions, especially
18 during the summer season. Recently, data from three high Arctic sites
19 (Zeppelin research station, Gruevbadet Observatory, Villum Research Station
20 at Station Nord) over a 3-year period (2013–2015) were analysed via
21 clustering analysis, reporting different categories including pristine low
22 concentrations (12 %–14 % occurrence), new particle formation (16 %–32 %),
23 Aitken (21 %–35 %) and accumulation (20 %–50 %) particles categories
24 (Dall'Osto et al., 2019). To our knowledge, this is the first year-long Antarctic
25 dataset where cluster analysis has been applied. The objective of this work is
26 to analyze different types of aerosol size distributions collected over a whole
27 year of measurements, to elucidate source regions (including open ocean,
28 land, snow on land, consolidated and marginal sea ice zones), discuss
29 possible primary and secondary aerosol components, and propose
30 mechanisms where NPF and growth may take place in the study region.

31
32
33
34

1
2
3
4
5
6
7
8
9
10
11
12
13
14
15
16
17
18
19
20
21
22
23
24
25
26
27
28
29
30
31
32
33

2. Methods

2.1 Location

The measurements reported here were made at the British Antarctic Survey's Halley VI station (75° 36'S, 26° 11'W), located in coastal Antarctica, on the floating Brunt Ice Shelf ~20 km from the coast of the Weddell Sea. A variety of measurements were made from the Clean Air Sector Laboratory (CASLab), which is located about 1 km south-east of the station (Jones et al., 2008).

2.2 SMPS and CPC

The aerosol size distribution was measured using a TSI Inc. Scanning Mobility Particle Sizer (SMPS), comprising an Electrostatic Classifier (model 3082), a Condensation Particle Counter (CPC) model 3775, and a long Differential Mobility Analyser (DMA, model 3081). The SMPS returned information on numbers of particles in discrete size bins in the size range 6 nm to 209 nm, at 1-min temporal resolution. A condensation particle counter (CPC, TSI Inc. model 3010) is routinely run at Halley. It provides a measure of total number of particles with diameter between 10 nm and ~3 microns. Both instruments sampled from the CASLab's central, isokinetic, aerosol stack (200 mm i.d. stainless steel) (see Jones et al. (2008) for details).

2.2.1. SMPS K means clustering data analysis

Cluster Analysis has routinely been used to understand SMPS data for over a decade (Dall'Osto et al (2019, 2018a, 2018b, 2018c, 2017, Lange et al 2018, Beddows et al 2014, 2009) and is useful in reducing the complexity of multivariate data into a manageable size to understand natural processes in the environment. The cluster analysis procedure is relatively straightforward and consists of three stages: (i) normalisation; (ii) cluster choice; and (iii) cluster partition.

- 1 (i) Prior to clustering, the SMPS distributions are normalized so that the
2 Euclidean length of each (treated as a vector) is 1. This ensures
3 that we are clustering the shape of the distributions irrespective of
4 the magnitude of the number count within each. The normalized
5 data given then are clustered using *k*-means (method R Core Team
6 (2019). This partitions the SMPS distributions (treated as vectors by
7 *k*-means) into *k* groups such that the sum of squares of the
8 distances from these points to the assigned cluster centres is
9 minimized. At the minimum, the cluster centres form the average
10 SMPS distributions of the individual SMPS distributions assigned to
11 each cluster (see supporting information in Beddows and Harrison,
12 2019 for more details).
- 13 (ii) The choice of cluster number can be decided upon using cluster
14 validation metrics which parameterise the compactness and
15 separation of the clusters within the measurements space (i.e. a
16 space with the same number of dimensions as the number of size
17 bins within the SMPS). In an ideal case, each cluster forms its own
18 island within the measurement space, defined by highly similar
19 elements (i.e. are compact) and are distinct from each other by
20 highly dissimilar elements (i.e. are separate). However, in the case
21 of SMPS spectra such a high degree of compactness and
22 separation is not realised in environmental data. Instead, the data is
23 partitioned into areas of increased density within the measurement
24 space, i.e. the data does not have sufficient compactness and
25 separation to form *islands* within the measurement space but
26 instead forms *hills* within the measurement *landscape*, which is
27 divided up by the partitions.

28

29 To decide on the number of factors, the Dunn Index (DI) and Silhouette
30 Width (SW) were calculated for each factor number (Halkidi et al 2001 and
31 Rousseeuw 1987). The DI is a function the ratio of the smallest distance
32 between observations not in the same cluster to the largest intra-cluster
33 distance. Hence, DI has a value of 0 and above. The higher the values
34 the more compact and separate are the elements within the clusters but

1 conversely the closer the value is to zero the more loose and diffuse the
2 elements are across the clusters. When cluster analysing SMPS data, a
3 DI of the order of 10^{-3} - 10^{-4} is often obtained indicating that *k*-Means is
4 partitioning the data into clusters which are in close proximity to each other.

5
6 The average SW value is a measure of how similar the observations are
7 with the clusters they are assigned to relative to other clusters. A value
8 approaching 1 indicates that the elements within each cluster are identical
9 to each other; a values close to 0 suggest that there is no clear division
10 between clusters; and a value to -1 suggest that elements are better
11 placed in its nearest neighbouring cluster. Typical values for SMPS data
12 are of the order 0.3 - 0.4, and coupled with the low DI value, indicate that
13 the clusters within the SMPS data are less compact and separate but
14 rather loose and diffuse (cf the analogy alluded to above of *hills within a*
15 *landscape* instead of *island within a sea*).

16
17 As we increase the cluster number from 2 up to 30, the SW value
18 decreases from a maximum value of 0.49 to 0.28 and the DI increases
19 from a minimum of 2.9×10^{-3} to a maximum 12.3×10^{-3} (Figure SI 1). As
20 the number of clusters is increased from 2, the increase in DI and
21 decrease in SW reflects the 'loose and diffuse' nature of the SMPS
22 elements within the clusters, i.e. as the number of clusters is increase, the
23 small irregularities within the data due to noise, are more likely to be
24 partitioned. Hence, we look for the cluster number (in this case 8 cluster;
25 with SW = 0.35 and DI = 4.6×10^{-3}) where there is a peak in this trend
26 identifying the natural partition within the data, which marks out the *islands*
27 of increased density space.

28
29 As with all statistical methods, there is a tendency to depend on the cluster
30 validation metrics to drive the final solution that may not necessarily be the
31 correct solution to describe the environmental conditions. Hence, they are
32 only used as a guide and it is often helpful as a next step to compare the
33 plots of the individual SMPS elements against the mean SMPS of each
34 cluster (Figure SI 2).

1
2
3
4
5
6
7
8
9
10
11
12
13
14
15
16
17
18
19
20
21
22
23
24
25
26
27
28
29
30
31
32
33
34

From figure SI 2, it is clear that we do indeed have sufficient separation of the SMPS data within the clusters with the odd spurious NSD in clusters 1, 3, 4 and 7, which are themselves insufficient in number to form their own cluster, but are allocated to their nearest cluster. From this optimum situation, it can be envisioned that as we reduce the number of clusters we will lose the integrity of the separation and we might well expect the cluster elements to aggregate into larger clusters according to their modal diameter, eg Clusters 1, 3, 4 and 7; clusters 2, 6 & 8; and cluster 6. In fact, when we calculate the median standard deviation of the SMPS data within the clusters for 2-10 clusters, there is in fact a minimum value at 8 clusters thus further supporting our cluster partitions.

2.3 Meteorological data

Standard meteorological measurements are made at the new Clean Air Sector Laboratory (CASLab) which is designed specifically for studies of background atmospheric chemistry and air/snow exchange, further information can be found elsewhere (Jones et al., 2008; Vignon et al., 2019).

2.4 Air mass trajectories

Air mass backtrajectories were calculated using the HYSPLIT4 trajectory model (Draxler and Hess, 1998) using the NCAR/NCEP 2.5-deg global reanalysis archive (Kalnay et al., 1996). Trajectories were calculated arriving at Halley (Lat. 75°34'16"S, Long. 25°28'26"W, 30m above sea level (asl)) every 6 hours (06:00, 12:00, 18:00, 00:00) during the study period. All calculations were carried out through the Openair trajectory functions in Cran R (Carslaw and Ropkins 2012). In particular, once calculated, the trajectories were clustered using the Openair function *trajCluster* using the Euclidean method. When considering the various cluster numbers, a setting of 6 trajectory clusters were chosen as best describing the air masses arriving at Halley. Note that metrics similar to the Dunn Index and Silhouette Width were not needed in this decision. The results of the air mass trajectory calculation

1 were plotted either as individual, average or raster layer objects (Hijmans
2 (2019)) drawn on stereographic projections of Antarctica using the *mapproj*
3 and *maps* package (Becker 2018, Doug McIlroy *et al* 2018).

4 5 **3. Results**

6 7 **3.1 Categorizing Antarctic aerosol size distributions**

8 9 **3.1.1 Average particle number and size resolved concentrations**

10
11 We investigated the seasonal variability in the physical aerosol size
12 characteristics of particles sampled from Halley VI Station in coastal
13 Antarctica over the period January to December 2015. A clear maximum at 45
14 nm and at 145 nm can be seen in the annual average size distribution (Fig. 1).
15 However, a striking difference can be seen among different seasons: high
16 concentrations of aerosols at about 40 nm dominate during summer, whereas
17 larger modes can be observed during winter; with intermediate conditions
18 during spring and autumn. The difference between spring and autumn at
19 $D > 60$ nm is also interesting, showing much higher concentrations in autumn,
20 and likely due to a number of additional unknown sources including primary
21 (sea spray and blowing snow) and secondary (sulphate and organic
22 components).

23
24 Results are broadly in line with previous results published from the Antarctic
25 Peninsula (Kim *et al.*, 2017). Total particle number concentrations are
26 derived from a condensation particle counter (CPC) deployed parallel to the
27 SMPS (Fig. SI 3), supporting the excellent performance of the SMPS over a
28 large data coverage (89% of the time during 2015). Minimum concentrations
29 are found for the month of August (47 ± 10 cm⁻³) and maximum for January
30 (602 ± 65 cm⁻³). These are reflected in the clear seasonal cycles for the total
31 particle concentration (CN) observed (Fig SI 4). Figure SI 4 (bottom) also
32 shows daily average concentrations of the $N_{30 \text{ nm}}$, $N_{30-100 \text{ nm}}$ and $N_{>100 \text{ nm}}$
33 integral particle population. The selected cutoffs of 30 and 100 nm are based

1 on the average shape of the size distribution (Figure 1). It is interesting that
2 whereas the absolute concentrations are remarkably different, the relative
3 percentages of the three aerosol populations do not differ much across
4 different months, on average $21\pm 9\%$, $54\pm 7\%$ and $25\pm 8\%$ for the $N_{30\text{ nm}}$, N_{30-100}
5 nm and $N_{>100\text{ nm}}$, respectively. Ultrafine particles dominate summer
6 concentrations, but are - relative to total - a dominating fraction also during
7 winter.

8

9 **3.1.2 K-means SMPS cluster analysis**

10

11 K-means cluster analysis of particle number size distributions was performed
12 using 5,664 hourly distributions collected over the year of 2015. Our clustering
13 analysis led to an optimum number of eight categories of aerosol number size
14 distributions. The corresponding average daily aerosol number size
15 distributions are shown in Figure 2a, whereas the annual seasonality is shown
16 in Figure 2b. Here, we refer to ultrafine as particles with diameters between 6
17 and 210 nm. Three categories were characterized by very low particle number
18 concentrations ($<200\text{ particles cm}^{-3}$), and described by their different aerosol
19 modes (plotted and size resolved in Fig. 3), specifically:

20

21 - "*Pristine_30*" ultrafine. Occurring annually 19% of the time (min-max 0-55%
22 based on monthly averages), this aerosol category ($N_{\text{CPC}} 179\pm 30\text{ cm}^{-3}$) shows
23 two main peaks at 30 nm and 95 nm (Fig. 3, Fig. SI 5). The maximum in
24 occurrence is seen for the months of September (47%) and May (55%).

25

26 - "*Pristine_75*" ultrafine. Occurring annually 29% of the time (min-max 0-61%
27 based on monthly averages), this aerosol category ($N_{\text{CPC}} 157\pm 25\text{ cm}^{-3}$) shows
28 two main peaks at 70 nm and 130 nm (Fig. 3, Fig. SI 5). The occurrence is
29 scattered across all year except during spring months (Sept/Oct).

30

31 - "*Pristine_160*" ultrafine. Occurring annually 9% of the time (min-max 0-52%
32 based on monthly averages), this aerosol category ($N_{\text{CPC}} 121\pm 40\text{ cm}^{-3}$) shows
33 two main peaks at 70 nm and 160 nm (Fig. 3, Fig. SI 5). The maximum in
34 occurrence is seen for the winter months of June (41%) and July (52%).

1

2 These three pristine aerosol cluster types describe up to 57% of the aerosol
3 population, and mainly dominate the aerosol population during cold months
4 (73%-100% for Apr-Aug.) Other aerosol categories possessing higher particle
5 concentrations include:

6

7 - "*Nucleation*" ultrafine. Occurring annually 3% of the time (min-max 0-11%
8 based on monthly averages), this aerosol category ($N_{CPC} 620 \pm 220 \text{ cm}^{-3}$)
9 shows a main nucleation peak at 15 nm detected during summer months (Fig.
10 2 a, b). Figure SI5d shows the evolution of the aerosol number size
11 distributions starting at about noon and peaking at about 18:00; overall 95% of
12 these events were detected during daylight. The name of this category - which
13 will be used below to represent new particle formation events - stands for
14 continuous gas-to-particle growth occurring after the particle nucleation event,
15 although these nucleation events - detected at about 7-10 nm - must have
16 originated away from the Halley station.

17

18 - "*Bursting*" ultrafine. Occurring annually 9% of the time (min-max 0-37%
19 based on monthly averages), this aerosol category ($N_{CPC} 602 \pm 120 \text{ cm}^{-3}$)
20 shows a main nucleation peak at 27 nm detected during summer months (Fig.
21 2a, b). Fig. SI5e suggests these aerosols are similar to the *Nucleation* cluster,
22 although these new particle formation events are already in the growth
23 process almost reaching 30 nm on average.

24

25 Clusters *Nucleation* and *Bursting* are seen during summer months and
26 September-October, contributing up to 44% of the total aerosol population
27 during the months of September and January (Fig. SI6b, d). Following
28 terminology developed in previous work (Dall'Osto et al., 2017, 2018) the
29 remaining aerosol clusters can be classified as followed:

30

31 - "*Nascent*" ultrafine. This category occurs annually 10% of the time, with a
32 strong seasonal trend peaking during summer (October-December, 10-39%)
33 and with a broad Aitken mode centred at about 38 nm (Fig.2) without showing
34 a clear diurnal pattern (Fig. SI5f). The name of this category emerges from

1 growing ultrafine aerosol particles which may result from an array of different
2 primary and secondary aerosol processes.

3

4 - "*Aitken*" ultrafine. This category occurs annually 15% of the time, with a
5 strong seasonal trend peaking during summer (Oct-Dec, 32-63%, Fig. 2b) and
6 - similar to the *Nascent* cluster - a broad Aitken mode centred at about 50 nm
7 (Fig 2a) without showing a clear diurnal pattern (Fig. SI 5h).

8

9 - "*Bimodal*" ultrafine. Occurring annually 5% (min-max 0-21%) of the time, this
10 unique category shows a strongly bimodal size distribution (43nm and 134nm,
11 with a small nucleation mode at 16 nm, Fig. 2 a), it occurs during the period
12 Dec-Apr (7-21%) and parallels previously reported bimodal aged Antarctic
13 distributions (Ito et al., 1993). The Hoppel minimum mode is seen at 70 nm.

14

15 In summary, our method allows apportionment of the Antarctic aerosol
16 observed at Halley research station into eight categories describing the whole
17 aerosol population. In the following sections, emphasis is given to
18 understanding the origin and processes driving Antarctic aerosol formation.

19

20 **3.2 Association of PSD with meteorological, physical and chemical** 21 **parameters**

22

23 The main ground-level meteorological observations from Halley for the year
24 2015 are temporally averaged over the periods of occurrence of the different
25 aerosol categories (Fig SI 7). Higher average wind speeds (WS, $7.2 \pm 2 \text{ m s}^{-1}$)
26 were encountered for the pristine aerosol clusters relative to the remaining
27 five ($3.2 \pm 2 \text{ m s}^{-1}$); cluster *pristine_160* shows the highest WS ($8.5 \pm 3 \text{ m s}^{-1}$),
28 suggesting the larger mode may be due to a primary aerosol component,
29 further discussed in Section 4. Little variation in atmospheric pressure was
30 found among the eight aerosol clusters. By contrast, *Nucleation* and *Bursting*
31 clusters were found in driest (Relative Humidity RH, $48 \pm 5\%$) and coldest (T -
32 $17 \pm 0.2 \text{ }^\circ\text{C}$) weather among all clusters, supporting the fact that NPF takes
33 place preferentially at low RH (Laaksonen et al.; 2009; Hamed et al. 2011).

1 Vertical profiles of meteorological data are available for most days in 2015,
2 and complement local ground-level measurements. Fig. SI6a-b show driest
3 and coldest conditions for clusters *Bursting* and *Nucleation*. By contrast,
4 warmest and wettest conditions occur for the *Bimodal* category. A large
5 difference is also seen in the wind speed vertical profiles (Fig. SI 8c), which
6 are strongest for cluster *pristine_160*, and a clear inversion is seen during the
7 *bimodal* cluster days. Concurrent ozone gas measurements (Fig. SI 7) show
8 lowest values for the cluster *bimodal* (18 ± 3 ppb), moderate for ultrafine
9 dominating clusters (24 ± 8 ppb), and higher values for pristine clusters (29 ± 5
10 ppb).

11

12 **3.3 Elucidating source regions by association of PSD clusters with air** 13 **mass back trajectories**

14

15 Throughout the studied period, hourly 120 h back trajectories were calculated
16 using the HYSPLIT4 model (Draxler and Hess, 1998). Figure 4 shows the
17 results of the air mass back trajectories calculated for Halley throughout 2015,
18 showing six main clusters. Broadly, two air trajectory clusters were associated
19 with anticyclonic conditions (clusters 2 and 6, up to 33.6% of air masses);
20 three clusters were associated with air masses coming from the East Antarctic
21 Plateau (clusters 3, 4, 5, up to 57.2% of air masses); and one unique air
22 trajectory cluster was found associated with air masses originating within the
23 Weddell Sea (cluster 1, 9%).

24 Fig. SI9 shows the six air mass back trajectory clusters and the average
25 height of the trajectories up to 120 hours before arrival at Halley. While
26 clusters 2-6 show their origin over the Antarctic plateau, cluster 1 shows
27 average altitudes lower than 1000m, close to the height of the mixed layer
28 (Fig. SI9). Figure SI 10 shows the air mass trajectories according to the PSD
29 clusters, On the basis of Figure SI9, it looks rather similar to the other air
30 mass types with the air only entering the boundary layer for the last ~15 hours
31 of the trajectory. One striking difference is found when these air mass back
32 trajectory clusters are compared temporally among the aerosol categories
33 (Figure 5).

1 A key conclusion of this study is that most aerosol categories (excluding
2 cluster *Nucleation*) are associated with air masses arriving with Eastern winds
3 from the Antarctic plateau (East short, East long, 56-76% of the time).
4 Anticyclones also seem to be a predominant air mass type (17-42%). At
5 Halley, air mass back trajectories that have travelled over the sea/sea ice
6 zone, play only a minor overall role in terms of annual average air mass
7 trajectories (10-15%).

8 In a further analysis, we obtained information on how far each air mass
9 travelled (total travel time 60 h) over zones distinguished by their surface
10 characteristics, namely snow, sea ice and open water for each one of the
11 different aerosol categories presented (see methods). Fig. 5a shows that
12 category *Nucleation* is the one most associated with sea ice (27% of the time).
13 An example of a NPF events is shown in Fig. SI 11, occurring on the 28th
14 January 2015, where air masses back trajectories showed most of their travel
15 time over sea ice (65% consolidate, 25% open pack, total 85%) and the
16 remaining open ocean (10%). Further studies will address specific events and
17 more specific case studies. It is important to stress that the *Nucleation*
18 category has its air mass back trajectories mainly travelling over land (63%).
19 However - relative to the other clusters - it is the most affected by air masses
20 which had travelled over the Weddell Sea (27%), most of which is open pack
21 ice (ratio open pack / consolidated sea ice of 0.6, Fig. 5b). This is an important
22 conclusion of this work, pointing out that at least two source regions of new
23 particle formation exist in the Antarctic. It is interesting to note also that the
24 *Bursting* category has a large ratio of open pack / consolidated sea ice (Fig
25 5b), confirming marginal sea ice zones may be a strong source of biogenic
26 gases responsible for new particle formation.

27 By examining the air mass trajectory heights, we also show that during the 5
28 days prior to sampling, the sampled air from the Weddell Sea was remarkably
29 different from the other air mass types (Fig. SI 9); it had travelled within the
30 marine boundary layer, with no intrusion from the free troposphere. Our
31 results strongly suggest the nucleating events originated within the boundary
32 layer, likely from gaseous precursors associated with sea ice emissions.

33
34

4. Discussion

4.1 Origin and sources of Antarctic aerosol

The purpose of this study was to analyze a year-long (throughout 2015) set of observations of Antarctic aerosol number size distributions to gain a better understanding of those processes which control Antarctic aerosol properties.

In a pristine environment like Antarctica and its surrounding ocean, where the atmosphere is thought to still resemble that of preindustrial Earth (Hamilton et al., 2014), missing aerosol sources must reflect overlooked natural processes. Uncertainties for modeling aerosol-cloud interactions and cloud radiative forcing arise from a poor source apportionment of aerosols and their size distributions (Carslaw et al 2013).

Broadly, marine particles in the nanometer size range originate from gas-to-particle secondary processes, whereas those in super-micron sizes are predominantly composed of primary sea-spray (O'Dowd et al., 1997). However, the accumulation mode (broadly composed of intermediate particle sizes of 50 –500 nm) is composed of a complex mixture of both secondary and primary particles. The relative roles of secondary aerosols produced from biogenic sulfur versus primary sea-spray aerosols in regulating cloud properties and amounts above the Southern Ocean is still a matter of debate (Meskhidze and Nenes, 2006; Korhonen et al., 2008; Quinn and Bates, 2011; Mc Coy et al., 2015; Gras and Keywood, 2017; Fossum et al., 2018). First observations of organic carbon (OC) in size-segregated aerosol samples collected at a coastal site in the Weddell Sea (Virkkula et al., 2006) showed that MSA represented only a few % of the total OC in the submicron fraction; recent studies demonstrate that sea bird colonies are also important sources of organic compounds locally (Schmale et al., 2013; Liu et al., 2018) and from seasonal ice microbiota (Dall'Osto et al., 2017). The overall balance between secondary aerosol formation versus primary particle formation from sea spray still needs to be determined and is a pressing open question.

1 A key result of this study is that for 59% of the year (89-100% during winter
2 JJA; 10-50% during spring SON; 34-65% during summer DJF; 48-91% during
3 autumn MAM), aerosol size distributions were characterized by very low
4 particle number concentrations ($< 121-179 \text{ cm}^{-3}$). It is often assumed that a
5 strong annual cycle of particle number concentrations is mainly driven by
6 summer new particle formation events (Shaw, 1988; Ito et al., 1993; Kerminen
7 et al., 2018). However, at Halley during summer 2015, 34-65% of the time low
8 particle number concentrations ($121-179 \text{ cm}^{-3}$) of unknown origin dominate
9 the overall temporal variation. Unique bimodal size distributions are seen in
10 December-April, where a clear bimodal distribution is seen for 7-21% of the
11 time (peaking in March, 21%), and likely related to cloud processing (Hoppel
12 et al., 1994).

13 In the following sub-sections we discuss our results in the light of recent
14 studies focusing on Antarctic aerosol source apportionment. The majority of
15 the studies report primary and secondary components in term of mass, which
16 should not be confused with particle number concentration.

17

18 **4.1.1 Primary Antarctic aerosol**

19

20 Sea spray is almost always reported as the main source of supermicron (>1
21 μm) aerosols in marine areas, including the Southern Ocean and Antarctica
22 (Quinn et al., 2015; Bertram et al., 2018). However, models of global sea-salt
23 distribution have frequently underestimated concentrations at polar locations
24 (Gong et al., 2002). Rankin and Wolff (2003) suggested the Antarctic sea ice
25 zone was a more important source of sea salt aerosol, during the winter
26 months, than the open ocean. In particular, they proposed brine and frost
27 flowers on the surface of newly forming sea ice as the dominant source, a
28 hypothesis supported by other studies (e.g. Udasti et al., 2012). The results
29 presented here suggest that, in coastal Antarctica, aerosol composition is a
30 strong function of wind speed and that the mechanisms determining aerosol
31 composition are likely linked to blowing snow (Giordano et al., 2019; Yang et
32 al., 2019; Frey et al., 2020). We note that Legrand et al. (2017a) suggested
33 that on average, the sea-ice and open-ocean emissions equally contribute to
34 sea-salt aerosol load of the inland Antarctic atmosphere.

1 Averaged across the year, we found a very clear aerosol size distribution with
2 the largest detected mode at ~160 nm, pointing to a primary - likely sea spray
3 - source, which was detected during periods of strong winds. However, it is
4 also possible that in size range the dominating constituent is sulphate (Teinilä
5 et al., 2014), further studies are needed to apportion this mode correctly. This
6 aerosol category type occurs very frequently during winter months (JJ, 33-
7 52%), but not during the other months (0-14%). Gras and Keywood (2017)
8 showed, using data from Cape Grim, that wind-generated coarse-mode sea
9 salt is an important CCN component year round and from autumn through to
10 mid-spring is the second most important component, contributing around 36%
11 to observed CCN; these measurements were taken in the Southern Ocean
12 marine boundary layer.

13 Marine primary organic aerosol (POA) is often associated with sea-spray, but
14 recent studies indicate that a fine mode (usually <200 nm) can have a size
15 distribution that is independent from sea-salt (externally mixed), whereas
16 supermicron marine aerosols are more likely to be internally mixed with sea-
17 salt (Gantt and Meskhidze, 2013). McCoy et al. (2015) reported observational
18 data indicating a significant spatial correlation between regions of elevated
19 Chl-a and particle number concentrations across the Southern Ocean, and
20 showed that modeled organic mass fraction and sulphate explains $53 \pm 22\%$
21 of the spatial variability in observed particle concentration. Our study cannot
22 apportion any aerosol related to primary organic aerosol, given the lack of
23 chemical measurements carried out during 2015 at Halley research station. It
24 is possible that part of the broad mode at 90 nm of the Pristine_90 category
25 contain a fraction of primary marine organic aerosols, but the relative
26 importance cannot be quantified in this study. Interestingly, open ocean
27 aerosol measurements collected over the Southern Ocean (43°S–70°S) and
28 the Amundsen Sea (70°S–75°S) were recently reported by Jung et al. (2019).
29 During the cruise, Water Insoluble Organic Components (WIOC) was the
30 dominant Organic Carbon (OC) species in both the Southern Ocean and the
31 Amundsen Sea, accounting for 75% and 73% of total aerosol organic carbon,
32 respectively. The WIOC concentrations were found to correlate with the
33 relative biomass of a specific phytoplankton species (*P. Antarctica*), producing

1 extracellular polysaccharide mucus and strongly affecting the atmospheric
2 WIOC concentration in the Amundsen Sea (Jung et al., 2019).

4 **4.1.2 Secondary Antarctic aerosol**

5
6 Our results show that two sub 30 nm aerosol categories (*Nucleation* and
7 *Bursting*, 12% in total) and two Aitken 30-60 nm aerosol categories (*Nascent*
8 and *Aitken*, 25%) account for up to 37% of the PSD detected during at Halley
9 the year 2015. Our results point to secondary aerosol processes driving the
10 aerosol population during five months of the year (Sep-Jan, 48-90%), where
11 aerosol particle number concentrations are on average 3-4 higher than the
12 Antarctic aerosol annual winter average concentration (121-179 cm⁻³). Our
13 study strongly suggests that new particle formation may have at least two
14 contrasting sources. The former is related to sea ice marginal zones formed in
15 the marine boundary layer. The latter is related to air masses arriving from the
16 Antarctic plateau, possibly having a free troposphere origin.

17 The biogenic precursors responsible for the new particle formation are not
18 known. Charlson et al. (1987) postulated the CLAW hypothesis - the most
19 significant source of CCN in the marine environment is non-sea-salt sulfate
20 derived from atmospheric oxidation of dimethylsulfide (DMS); however
21 measurements able to provide information on where individual particles come
22 from are still limited (O'Dowd et al., 1997b; Quinn and Bates, 2011; Sanchez
23 et al., 2018). A previous ship-borne field campaign in the Weddell Sea found
24 increased new particle formation in the sea ice zone of the Weddell Sea
25 (Davison et al., 1996), but no clear correlation to the dimethyl sulphide that
26 was then assumed to control new particle bursts. A smaller mode radius
27 associated with polar aerosol (relative to marine Southern ocean aerosol) was
28 found associated with less cloud cover, and consequently less cloud
29 processing, over the continent and pack ice regions. During the cruise, new
30 particle formation observed over the Weddell Sea, resulted from boundary
31 layer nucleation bursts rather than tropospheric entrainment. Brooks and
32 Thornton (2018) argued that additional modeling studies are still needed that
33 address contributions from both secondary DMS-derived aerosols and primary
34 organic aerosols as CCNs on realistic timescales; although the occurrence of

1 a “seasonal CLAW” in remote marine atmospheres is becoming plausible
2 (Vallina and Simó, 2007; Quinn et al., 2017; Sanchez et al., 2018).
3
4 Satellite (Schonhardt et al., 2008) and on-site measurements (Saiz-Lopez et
5 al., 2007; Atkinson et al., 2012) showed that the Weddell Sea is an iodine
6 hotspot; however there was no short-term correlation between IO and particle
7 concentration found (Roscoe et al., 2015). Using an unprecedented suite of
8 instruments, Jokinen et al. (2018) showed that ion-induced nucleation of
9 sulfuric acid and ammonia, followed by sulfuric acid–driven growth, is the
10 predominant mechanism for NPF and growth in eastern Antarctica a few
11 hundred kilometers from the coast (Finnish Antarctic research station (Aboa)
12 is located at the Queen Maud land, Eastern Antarctica; Jokinen et al., 2018).
13 Some ion clusters contained iodic acid, but its concentration was very small,
14 and no pure iodic acid or iodine oxide clusters were detected (Sipila et al.,
15 2016). Finally, some organic oxidation products from land melt ponds have
16 also been suggested (Kyro et al., 2013) as a potential source for condensable
17 vapor, although this may be a confined and minor source (Weller et al., 2018).
18 Other measurements of new particle formation and growth were governed by
19 the availability of other yet unidentified gaseous precursors, most probably low
20 volatile organic compounds of marine origin (Weller et al., 2015; 2018).

21

22 **4.2 Implication for climate and conclusion**

23

24 A strong annual cycle of total particle number concentration is a prominent
25 characteristic of the Antarctic aerosol system, with the austral summer
26 concentration being up to 20-100 times greater than during the winter (Shaw
27 1988, Gras 1993, Ito 1993, Hara et al 2011, Weller et al 2011, Järvinen et al
28 2013, Fiebig et al 2014, Kim et al 2017). These summer particle number
29 concentration maxima are largely explained by NPF taking place in the
30 Antarctic atmosphere. However, these seasonal cycles are more pronounced
31 at monitoring sites situated on the upper plateau of Antarctica than at the
32 coastal Antarctic sites. It is worth to keep in mind that these cycles could also
33 be more pronounced because in coastal regions in winter, sea salt aerosol

1 has a relatively larger source. i.e. the amplitude of the seasonal is driven both
2 by what is going on in winter as well as summer. Nevertheless, overall much
3 higher particle number concentrations have long been reported in coastal
4 Antarctica relative to the plateau. The vertical location of Antarctic NPF has
5 not been well quantified; there are some indications that NPF takes place
6 preferentially in the Antarctic Free Troposphere (FT) rather than in the
7 Boundary Layer (BL) (Koponen et al 2002, Hara et al 2011, Humphries et al
8 2016), whereas other studies shows opposite trends (Kim et al., 2017, Weller
9 et al., 2011; 2013; 2018). A study conducted on the upper plateau of
10 Antarctica demonstrates that also wintertime regional NPF is possible in this
11 environment (Järvinen et al 2013). Very low particle growth rates (between
12 about 0.1 and 1 nm h⁻¹) were reported in Antarctica (Park et al 2004, Weller et
13 al 2015).

14

15 We obtained data from Dome C and King Sejong (KS) Station for the period
16 May-December 2015, and compared them with Halley (H). Data are shown in
17 Fig. 6 where seasonal mean aerosol size distributions measured
18 simultaneously at three different sites are reported for (a) May-December
19 2015 (8 months in total); (b) Spring (September, October, November, 3
20 months in total); (c) Summer (December, 1 month in total) and (d) Winter
21 (June, July, August, 3 months in total, a map of the three stations considered
22 is shown in Figure 7. Overall, much higher concentrations are seen at the
23 coastal Antarctic sites (H, KS stations) relative to Dome C station (Fig. 6a).
24 The presence of permanent Antarctic stations could also affect aerosol size
25 distributions (Kim et al., 2017), future studies will aim at comparing aerosol
26 size distributions data simultaneously collected in different Antarctic stations.
27 Two broad modes at about 30-50 nm and at about 110-160 nm can be seen
28 for the coastal stations, whereas a smaller single mode at 60 nm is seen for
29 the Dome C station. When three seasons are compared, very different
30 features can be seen. During spring (Fig. 6b), both Aitken and accumulation
31 modes dominate the coastal sites, whereas a strong single mode is seen in
32 the Dome C site. By contrast, during summer (Fig. 6c), much stronger
33 nucleation and Aitken modes are seen at the coastal sites, likely due to NPF
34 taking place during summer time. The smaller nucleation mode size detected

1 in the Antarctic peninsula (King Sejong Station) relative to the one seen at
2 Halley may suggest a more local source of NPF in the Antarctic peninsula,
3 including open water, coastal macroalgae, and bird colonies. The average
4 size distributions during winter (Fig. 6d) again show marked differences
5 among the three different monitoring sites. Halley stations shows the largest
6 aerosol modes (about 100 nm and 160 nm), whereas smaller modes can be
7 seen at the other two sites. Overall, Fig. 6 serves to stress that the aerosol
8 population in Antarctica - an environment often considered homogenous and
9 simple to study - is different in different geographical regions, and very likely a
10 number of different processes and sources affect the aerosol population at
11 different times of the year. Ito et al. (1993) presented a conceptual diagram,
12 where different aerosol size distributions were seen, and a main NPF mode
13 was associated with the free troposphere and transported by katabatic winds.
14 Korhonen et al. (2008) also estimated that over 90% of the non-sea spray
15 CCN were generated above the boundary layer by nucleation of sulfuric acid
16 aerosol in the free troposphere. Our results point to sea ice regions and open
17 ocean water being a source not only of gaseous precursors, but also of new
18 particle formation, which then can growth once lifted in the free troposphere
19 (Fig. 8), and then larger modes are brought down again by the Antarctic
20 Drainage flow (James, 1989). The relative importance of free troposphere
21 versus boundary layer nucleation is not known at this stage, but this study
22 shows that the latter is seen, and the former is likely to happen and contribute
23 to the Aitken mode detected from the Antarctic plateau. Sea ice regions
24 (mainly via secondary processes, but also to a lesser degree via sea spray
25 and blowing snow) may control the CCN production, both regulating the first
26 stage of nucleation events and providing gaseous precursors, and slowly
27 growing nucleated particles with transport in the upper troposphere.

28

29 These results are in line with previous studies in polar areas. First, Dall'Osto
30 et al (2017) suggested that the microbiota of sea ice and sea ice-influenced
31 ocean were a significant source of atmospheric nucleating particles
32 concentrations (N_{1-3nm}). Second, within two different Arctic locations, across
33 large temporal scales (2000-2016) new particle formation was associated with
34 air mass back trajectories passing over open water and melting sea ice

1 regions, also pointing to marine biological activities within the open leads in
2 the pack ice and/or along the melting marginal sea ice zone (MIZ) being
3 responsible for such events (Dall'Osto et al., 2017b, Dall'Osto et al., 2018).
4 Our data from Halley, and the brief intercomparison with two other stations,
5 suggest that the size distributions of Antarctic submicron aerosols may have
6 been oversimplified in the past (Ito et al., 1993); and complex interactions
7 between multiple ecosystems, coupled with different atmospheric circulation,
8 result in very different aerosol size distributions populating the Southern
9 Hemisphere. We simply know too little about the sources of primary and
10 secondary aerosols of biogenic origin. Further studies are needed in order to
11 quantify the baseline aerosol properties in the polar regions and how they are
12 affected by emission processes and atmospheric processing and aging.
13 Future work in preparation will soon address these questions by an analysis of
14 aerosol size distributions simultaneously detected around the Antarctic
15 continent.

16

17 *Data availability.* Data can be accessed by contacting the corresponding
18 author.

19

20 *Supplement.* The supplement related to this article is available online.

21

22 *Author contributions.* DB and MD conducted the analysis and wrote the
23 manuscript. TCL, NB and AJ provided the Halley SMPS data. AL, YJY, AV
24 provided additional SMPS data. All authors edited and contributed to
25 subsequent drafts of the manuscript.

26

27 *Competing interests.* The authors declare that they have no conflicts of
28 interest.

29

30 *Financial support.* The study was further supported by the Spanish Ministry of
31 Economy through project PI-ICE (CTM 2017–89117-R) and the Ramon y
32 Cajal fellowship (RYC-2012-11922). The National Centre for Atmospheric
33 Science NCAS Birmingham group is funded by the UK Natural Environment
34 Research Council. AV was supported by the Academy of Finland's Centre of

1 Excellence program (Centre of Excellence in Atmospheric Science – From
2 Molecular and Biological processes to The Global Climate, project no.
3 272041). KS station SMPS measurement was supported by KOPRI project
4 (PE19010).

5

6 *Acknowledgements.* The authors are grateful to the overwintering staff at
7 Halley station who carried out the suite of measurements presented here. This
8 work was funded by the Natural Environment Research Council as part of the
9 British Antarctic Survey’s research programme “Polar Science for Planet
10 Earth”. We thank We thank Dr. Pasi Aalto (Institute for Atmospheric and Earth
11 System Research, University of Helsinki) and the joint French–Italian
12 Concordia Program with the project LTCPAA, for providing DMPS data of
13 2015 for intercomparison with data taken at Halley Station, similar data were
14 discussed in details elsewhere (Järvinen et al., 2013; Kim et al., 2017) .

15

16 *Review statement.* This paper was edited by Veli-Matti Kerminen and
17 reviewed by three anonymous referees.

18

19

20

21

22

23 **References**

24

25

26 Asmi, E., Frey, A., Virkkula, A., Ehn, M., Manninen, H., Timonen, H., Tolonen-
27 Kivimäki, O., Aurela, M., Hillamo, R., and Kulmala, M.: Hygroscopicity and
28 chemical composition of Antarctic sub-micrometre aerosol particles and
29 observations of new particle formation, *Atmos. Chem. Phys.*, 10, 4253–4271,
30 <https://doi.org/10.5194/acp-10-4253-2010>, 2010.

31

32

33 Atkinson, H. M., R.-J. Huang, R. Chance, H. K. Roscoe, C. Hughes, B. avison,
34 A. Schönhardt, A. S. Mahajan, A. Saiz-Lopez, and P. S. Liss (2012), Iodine
35 emissions from the sea ice of the Weddell Sea, *Atmos. Chem. Phys.*, 12,
36 11,229–11,244, doi:10.5194/acp-12-11229-2012.

37

38 Becagli, S., Scarchilli, C., Traversi, R., Dayan, U., Severi, M., Frosini, D.,
39 Vitale, V., Mazzola, M., Lupi, A., Nava, S., and Udisti, R.: Study of present-day
40 sources and transport processes affecting oxidised sulphur compounds in

1 atmospheric aerosols at Dome C (Antarctica) from yearround sampling
2 campaigns, Atmos. Environ., 52, 98–108,
3 <https://doi.org/10.1016/j.atmosenv.2011.07.053>, 2012.
4
5 Beddows, D. C. S., Dall'Osto, M., and Harrison, R. M.: Cluster Analysis of
6 Rural, Urban and Curbside Atmospheric Particle Size Data, Environ. Sci.
7 Technol., 43, 4694–4700, 2009.
8
9 Beddows, D. C. S., Dall'Osto, M., Harrison, R. M., Kulmala, M., Asmi, A.,
10 Wiedensohler, A., Laj, P., Fjaeraa, A. M., Sellegri, K., Birmili, W., Bukowiecki,
11 N., Weingartner, E., Baltensperger, U., Zdimal, V., Zikova, N., Putaud, J.-P.,
12 Marinoni, A., Tunved, P., Hansson, H.-C., Fiebig, M., Kivekäs, N., Swietlicki, E.,
13 Lihavainen, H., Asmi, E., Ulevicius, V., Aalto, P. P., Mihalopoulos, N., Kalivitis,
14 N., Kalapov, I., Kiss, G., de Leeuw, G., Henzing, B., O'Dowd, C., Jennings, S.
15 G., Flentje, H., Meinhardt, F., Ries, L., Denier van der Gon, H. A. C., and
16 Visschedijk, A. J. H.: Variations in tropospheric submicron particle size
17 distributions across the European continent 2008–2009, Atmos. Chem. Phys.,
18 14, 4327–4348, <https://doi.org/10.5194/acp-14-4327-2014>, 2014.
19
20 Beddows, D. C. S. and Harrison, R. M.: Receptor modelling of both particle
21 composition and size distribution from a background site in London, UK – a
22 two-step approach, Atmos. Chem. Phys., 19, 4863–4876,
23 <https://doi.org/10.5194/acp-19-4863-2019>, 2019.
24
25 Bertram, T.H.; Cochran, R.E.; Grassian, V.H.; Stone, E.A. Sea spray aerosol
26 chemical composition: Elemental and molecular mimics for laboratory studies
27 of heterogeneous and multiphase reactions. Chem. Soc. Rev.
28 2018, 47, 2374–2400
29
30 Boucher, O., Randall, D., Artaxo, P., Bretherton, C., Feingold, G., Forster, P.,
31 Kerminen, V. M., Kondo, Y., Liao, H., Lohmann, U., Rasch, P., Satheesh, S.,
32 Sherwood, S., Stevens, B., and Zhang, X.: Clouds and aerosols, in: Climate
33 change 2013: the physical science basis. Contribution of working group I to
34 the fifth assessment report of the intergovernmental panel on climate change,
35 edited by: Stocker, T. F., Qin, D., Plattner, G. K., Tignor, M., Allen, S.,
36 Boschung, J., Nauels, A., Xia, Y., Bex, V., and Midgley, P., chap. 7,
37 Cambridge University Press, Cambridge, 2013.
38
39 Brooks, S. D. and Thornton, D. C. O.: Marine Aerosols and Clouds,
40 Annu. Rev. Mar. Sci., 10, 289–313, 2018
41
42 Carslaw, K. S., Lee, L. A., Reddington, C. L., Pringle, K. J., Rap, A., Forster, P.
43 M., Mann, G.W., Spracklen, D. V., Woodhouse, M. T., Regayre, L. A., and
44 Pierce, J. R.: Large contribution of natural aerosols to uncertainty in indirect
45 forcing,
46
47 Carslaw, D. C. and K. Ropkins, (2012) openair --- an R package for air quality
48 data analysis. Environmental Modelling & Software. Volume 27-28, 52-61.
49 [10.1016/j.envsoft.2011.09.008](https://doi.org/10.1016/j.envsoft.2011.09.008)
50

1 Charlson, R. J., Lovelock, J. E., Andreae, M. O., and Warren, S. G.: Oceanic
2 Phytoplankton, Atmospheric Sulfur, Cloud Albedo and Climate, *Nature*, 326,
3 655–661, <https://doi.org/10.1038/326655a0>, 1987.
4
5 Chen, J. L., C. R. Wilson, D. Blankenship, and B. D. Tapley
6 2009), Accelerated Antarctic ice loss from satellite gravity
7 measurements, *Nat. Geosci.*, 2, 859–862, doi:10.1038/ngeo694.
8
9 Dall'Osto, M., Monahan, C., Greaney, R., Beddows, D. C. S., Harrison, R. M.,
10 Ceburnis, D., and O'Dowd, C. D.: A statistical analysis of North East Atlantic
11 (submicron) aerosol size distributions, *Atmos. Chem. Phys.*, 11, 12567–12578,
12 <https://doi.org/10.5194/acp-11-12567-2011>, 2011.
13
14 Dall'Osto, M., Beddows, D. C. S., Tunved, P., Krejci, R., Ström, J., Hansson,
15 H.-C., Yoon, Y. J., Park, K.-T., Becagli, S., Udisti, R., Onasch, T., O'Dowd, C.
16 D., Simó, R., and Harrison, R. M.: Arctic sea ice melt leads to atmospheric new
17 particle formation, *Sci. Rep.*, 7, 3318, [https://doi.org/10.1038/s41598-017-](https://doi.org/10.1038/s41598-017-03328-1)
18 [03328-1](https://doi.org/10.1038/s41598-017-03328-1), 2017a
19
20 Dall'Osto, M., Ovadnevaite, J., Paglione, M., Beddows, D. C. S., Ceburnis, D.,
21 Cree, C., Cortes, P., Zamanillo, M., Nunes, S. O., Perez, G. L., Ortega-
22 Retuerta, E., Emelianov, M., Vaque, D., Marrase, C., Estrada, M., Sala, M. M.,
23 Vidal, M., Fitzsimons, M. F., Beale, R., Airs, R., Rinaldi, M., Decesari, S.,
24 Facchini, M. C., Harrison, R. M., O'Dowd, C., and Simo, R.: Antarctic sea
25 ice region as a source of biogenic organic nitrogen in aerosols, *Scientific*
26 *Reports*, 7, 6047, [https://doi.org/10.1038/s41598-017-](https://doi.org/10.1038/s41598-017-06188-x)
27 [06188-x](https://doi.org/10.1038/s41598-017-06188-x), 2017b
28
29
30 Dall'Osto, M., Beddows, D. C. S., Asmi, A., Poulain, L., Hao, L., Freney, E.,
31 Allan, J. D., Canagaratna, M., Crippa, M., Bianchi, F., de Leeuw, G., Eriksson,
32 A., Swietlicki, E., Hansson, H. C., Henzing, J. S., Granier, C., Zemann, K.,
33 Laj, P., Onasch, T., Prevot, A., Putaud, J. P., Sellegri, K., Vidal, M., Virtanen,
34 A., Simo, R., Worsnop, D., O'Dowd, C., Kulmala, M., and Harrison, R. M.:
35 Novel insights on new particle formation derived from a paneuropean
36 observing system, *Sci. Rep.*, 8, 1482, [https://doi.org/10.1038/s41598-017-](https://doi.org/10.1038/s41598-017-17343-9)
37 [17343-9](https://doi.org/10.1038/s41598-017-17343-9), 2018a.
38
39 Dall'Osto, M., Geels, C., Beddows, D. C. S., Boertmann, D., Lange, R.,
40 Nøjgaard, J. K., Harrison Roy, M., Simo, R., Skov, H., Massling, A. Regions of
41 open water and melting sea ice drive new particle formation in North East
42 Greenland. *Sci. Rep.* 8, 6109., 2018b
43
44 Dall'Osto, M., Beddows, D. C. S., Tunved, P., Harrison, R. M., Lupi, A., Vitale,
45 V., Becagli, S., Traversi, R., Park, K.-T., Yoon, Y. J., Massling, A., Skov, H.,
46 Lange, R., Strom, J., and Krejci, R.: Simultaneous measurements of aerosol
47 size distributions at three sites in the European high Arctic, *Atmos. Chem.*
48 *Phys.*, 19, 7377–7395, <https://doi.org/10.5194/acp-19-7377-2019>, 2019.
49
50

1 Davison, B., O'Dowd C., Hewitt Cc, Smith M, Harrison Roy M, Peel D., Wolf E.,
2 Mulvaney R., Schwikowski M. and Baltensperger U., Dimethylsulfide and its
3 oxidation products in the atmosphere of the Atlantic and southern oceans,
4 *Atmos. Environ.*, 30, 1895-1906, 1996.
5
6 Doug McIlroy. Packaged for R by Ray Brownrigg, Thomas P Minka and
7 transition to Plan 9 codebase by Roger Bivand. (2018). mapproj: Map
8 Projections. R package version 1.2.6. [https://CRAN.R-](https://CRAN.R-project.org/package=mapproj)
9 [project.org/package=mapproj](https://CRAN.R-project.org/package=mapproj)
10
11 Draxler, R.R., and B.J.B. Stunder, 1988. Modeling the CAPTEX vertical tracer
12 concentration profiles. *J. Appl. Meteorol.*, , 27, 617-625.
13
14 Fiebig, M., Hirdman, D., Lunder, C. R., Ogren, J. A., Solberg, S., Stohl, A.,
15 and Thompson, R. L.: Annual cycle of Antarctic baseline aerosol: controlled by
16 photooxidation-limited aerosol formation, *Atmos. Chem. Phys.*, 14, 3083-3093,
17 <https://doi.org/10.5194/acp-14-3083-2014>, 2014.
18
19 Frey, M. M., Norris, S. J., Brooks, I. M., Anderson, P. S., Nishimura, K., Yang,
20 X., Jones, A. E., Nerentorp Mastromonaco, M. G., Jones, D. H., and Wolff, E.
21 W.: First direct observation of sea salt aerosol production from blowing snow
22 above sea ice, *Atmos. Chem. Phys.*, 20, 2549–2578,
23 <https://doi.org/10.5194/acp-20-2549-2020>, 2020.
24
25 Fossum, K. N., Ovadnevaite, J., Ceburnis, D., Dall'Osto, M., Marullo, S.,
26 Bellacicco, M., Simó, R., Liu, D., Flynn, M., Zuend, A., O'Dowd, C.:
27 Summertime primary and secondary contributions to Southern Ocean cloud
28 condensation nuclei, *Scientific Reports.*, 8, 13844, 2018.
29
30 Galí, M., Lévassieur, M., Devred, E., Simó, R., and Babin, M.: Sea-surface
31 dimethylsulfide (DMS) concentration from satellite data at global and regional
32 scales, *Biogeosciences*, 15, 3497-3519, [https://doi.org/10.5194/bg-15-3497-](https://doi.org/10.5194/bg-15-3497-2018)
33 [2018](https://doi.org/10.5194/bg-15-3497-2018), 2018.
34
35 Gantt, B. and Meskhidze, N.: The physical and chemical characteristics of
36 marine primary organic aerosol: a review, *Atmos. Chem. Phys.*, 13, 3979–
37 3996, [doi:10.5194/acp-13-3979-2013](https://doi.org/10.5194/acp-13-3979-2013), 2013.
38
39 Giordano, M. R., Kalnajs, L. E., Avery, A., Goetz, J. D., Davis, S. M., and
40 DeCarlo, P. F.: A missing source of aerosols in Antarctica – beyond long-
41 range transport, phytoplankton, and photochemistry, *Atmos. Chem. Phys.*, 17,
42 1–20, [https://doi.org/10.5194/acp-](https://doi.org/10.5194/acp-17-1-2017)
43 [17-1-2017](https://doi.org/10.5194/acp-17-1-2017), 2017
44
45 Giordano, M. R., Kalnajs, L. E., Goetz, J. D., Avery, A. M., Katz, E., May, N.
46 W., Leemon, A., Mattson, C., Pratt, K. A., and DeCarlo, P. F.: The importance
47 of blowing snow to halogen-containing aerosol in coastal Antarctica: influence
48 of source region versus wind speed, *Atmos. Chem. Phys.*, 18, 16689–16711,
49 <https://doi.org/10.5194/acp-18-16689-2018>, 2018.
50

1 Gras, J. L. and Keywood, M.: Cloud condensation nuclei over the Southern
2 Ocean: wind dependence and seasonal cycles, *Atmos. Chem. Phys.*, 17,
3 4419–4432, <https://doi.org/10.5194/acp-17-4419-2017>, 2017.
4
5 Halkidi, M., Batistakis, Y., Vazirgiannis, M., (2001) On Clustering Validation
6 Techniques, *Journal of Intelligent Information Systems*, 17:2/3, 107–145.
7
8 Hamed, A., Korhonen, H., Sihto, S.-L., Joutsensaari, J., Jarvinen, H., Petaja,
9 T., Arnold, F., Nieminen, T., Kulmala, M., Smith, J. N., Lehtinen, K. E. J., and
10 Laaksonen, A.: The role of relative humidity in continental new particle
11 formation, *J. Geophys. Res.*, 116, D03202, doi:10.1029/2010JD014186, 2011.
12
13 Hamilton, D. S., L. A. Lee, K. J. Pringle, C. L. Reddington, D. V. Spracklen,
14 and K. S. Carslaw, Occurrence of pristine aerosol environments on a polluted
15 planet, *P Natl Acad Sci USA*, 111, 18466–18471,
16 doi:10.1073/pnas.1415440111, 2014
17
18 Hara K, Osada K, Nishita-Hara Cand Yamanouchi T 2011 Seasonal variations
19 and vertical features of aerosol particles in the Antarctic troposphere *Atmos.*
20 *Chem. Phys.* 11 5471–84
21
22 Herenz, P., Wex, H., Mangold, A., Laffineur, Q., Gorodetskaya, I. V., Fleming,
23 Z. L., Panagi, M., and Stratmann, F.: CCN measurements at the Princess
24 Elisabeth Antarctica research station during three austral summers, *Atmos.*
25 *Chem. Phys.*, 19, 275–294, <https://doi.org/10.5194/acp-19-275-2019>, 2019.
26
27 Hodshire A L et al 2016 Multiple new-particle growth pathways observed at
28 the USDOESouthern Great Plains field site *Atmos. Chem. Phys.* 16 9321–48
29
30 Hoppel, W.A., Frick, G.M., Fitzgerald, J.W., 1994. Marine boundary layer
31 measurements of new-particle formation and the effects of non-precipitating
32 clouds have on aerosol size distribution. *J. Geophys. Res.* 99, 14443–14459
33
34 Humphries, R. S., Schofield, R., Keywood, M. D., Ward, J., Pierce, J. R.,
35 Gionfriddo, C. M., Tate, M. T., Krabbenhoft, D. P., Galbally, I. E., Molloy, S. B.,
36 Klekociuk, A. R., Johnston, P. V., Kreher, K., Thomas, A. J., Robinson, A. D.,
37 Harris, N. R. P., Johnson, R., and Wilson, S. R.: Boundary layer new particle
38 formation over East Antarctic sea ice – possible Hg-driven nucleation?, *Atmos.*
39 *Chem. Phys.*, 15, 13339–13364, <https://doi.org/10.5194/acp-15-13339-2015>,
40 2015.
41
42 Huang, J., Jaeglé, L., and Shah, V.: Using CALIOP to constrain blowing snow
43 emissions of sea salt aerosols over Arctic and Antarctic sea ice, *Atmos. Chem.*
44 *Phys.*, 18, 16253–16269, <https://doi.org/10.5194/acp-18-16253-2018>, 2018.
45
46
47 Ito T 1993 Size distribution of Antarctic submicron aerosols *Tellus B*
48 45 145–59
49

1 Jang, E., Park, K.-T., Yoon, Y. J., Kim, T.-W., Hong, S.-B., Becagli, S., raversi,
2 R., Kim, J., and Gim, Y.: New particle formation events observed at the King
3 Sejong Station, Antarctic Peninsula – Part 2: Link with the oceanic biological
4 activities, *Atmos. Chem. Phys.*, 19, 7595–7608, [https://doi.org/10.5194/acp-](https://doi.org/10.5194/acp-19-7595-2019)
5 [19-7595-2019](https://doi.org/10.5194/acp-19-7595-2019), 2019.
6
7 Järvinen, E., Virkkula, A., Nieminen, T., Aalto, P. P., Asmi, E., Lanconelli,
8 C., Busetto, M., Lupi, A., Schioppo, R., Vitale, V., Mazzola, M., Petäjä, T.,
9 Kerminen, V.-M., and Kulmala, M.: Seasonal cycle and modal structure of
10 particle number size distribution at Dome C, Antarctica, *Atmos. Chem. Phys.*,
11 13, 7473–7487, <https://doi.org/10.5194/acp-13-7473-2013>, 2013.
12
13 Jokinen, T., Sipilä, M., Kontkanen, J., Vakkari, V., Tisler, P., Duplissy, E.-M.,
14 Junninen, H., Kangasluoma, J., Manninen, H. E., Petäjä, T., Kulmala,
15 M., Worsnop, D. R., Kirkby, J., Virkkula, A., and Kerminen, V.-M.: Ion-induced
16 sulfuric acid–ammonia nucleation drives particle formation in coastal
17 Antarctica, *Sci. Adv.*, 4, eaat9744, <https://doi.org/10.1126/sciadv.aat9744>,
18 2018.
19
20 Jones, A. E., Wolff, E. W., Salmon, R. A., Bauguitte, S. J.-B., Roscoe, H. K.,
21 Anderson, P. S., Ames, D., Clemmshaw, K. C., Fleming, Z. L., Bloss, W. J.,
22 Heard, D. E., Lee, J. D., Read, K. A., Hamer, P., Shallcross, D. E., Jackson, A.
23 V., Walker, S. L., Lewis, A. C., Mills, G. P., Plane, J. M. C., Saiz-Lopez, A.,
24 Sturges, W. T., and Worton, D. R.: Chemistry of the Antarctic Boundary Layer
25 and the Interface with Snow: an overview of the CHABLIS campaign, *Atmos.*
26 *Chem. Phys.*, 8, 3789–3803, <https://doi.org/10.5194/acp-8-3789-2008>, 2008.
27
28 Jung, J., Hong, S.-B., Chen, M., Hur, J., Jiao, L., Lee, Y., Park, K., Hahm, D.,
29 Choi, J.-O., Yang, E. J., Park, J., Kim, T.-W., and Lee, S.: Characteristics of
30 biogenically-derived aerosols over the Amundsen Sea, Antarctica, *Atmos.*
31 *Chem. Phys. Discuss.*, <https://doi.org/10.5194/acp-2019-133>, in review, 2019.
32
33 Kalnay E., M. Kanamitsu, R. Kistler, W. Collins, D. Deaven, L. Gandin, M.
34 Iredell, S. Saha, G. White, J. Woollen, Y. Zhu, M. Chelliah, W. Ebisuzaki, W.
35 Higgins, J. Janowiak, K.C. Mo, C. Ropelewski, J. Wang, A. Leetmaa, R.
36 Reynolds, R. Jenne, D. Joseph The NCEP/NCAR 40-year Reanalysis project
37 *Bull. Am. Met. Soc.*, 77, pp. 437-471. [http://dx.doi.org/10.1175/1520-](http://dx.doi.org/10.1175/1520-0477(1996)077<0437:TNYR>2.0.CO;2)
38 [0477\(1996\)077<0437:TNYR>2.0.CO;2](http://dx.doi.org/10.1175/1520-0477(1996)077<0437:TNYR>2.0.CO;2), 1996
39
40 Kerminen, V.-M., Chen, X., Vakkari, V., Petäjä, T., Kulmala, M., and Bianchi,
41 F.: Atmospheric new particle formation and growth: review of field observations,
42 *Environ. Res. Lett.*, 13, 103003, <https://doi.org/10.1088/1748-9326/aadf3c>,
43 2018.
44
45 Kim, J., Yoon, Y. J., Gim, Y., Kang, H. J., Choi, J. H., Park, K.-T., and Lee, B.
46 Y.: Seasonal variations in physical characteristics of aerosol particles at the
47 King Sejong Station, Antarctic Peninsula, *Atmos. Chem. Phys.*, 17, 12985–
48 12999, <https://doi.org/10.5194/acp-17-12985-2017>, 2017.
49

- 1 Kim, J., Yoon, Y. J., Gim, Y., Choi, J. H., Kang, H. J., Park, K.-T., Park, J., and
2 Lee, B. Y.: New particle formation events observed at King Sejong Station,
3 Antarctic Peninsula – Part 1: Physical characteristics and contribution to cloud
4 condensation nuclei, *Atmos. Chem. Phys.*, 19, 7583–7594,
5 <https://doi.org/10.5194/acp-19-7583-2019>, 2019.
6
- 7 Kyrö, E.-M., Kerminen, V.-M., Virkkula, A., Dal Maso, M., Parshintsev, J.,
8 Ruíz-Jimenez, J., Forsström, L., Manninen, H. E., Riekkola, M.-L., Heinonen,
9 P., and Kulmala, M.: Antarctic new particle formation from continental biogenic
10 precursors, *Atmos. Chem. Phys.*, 13, 3527–3546, <https://doi.org/10.5194/acp-13-3527-2013>, 2013.
11
- 12
- 13 Koponen IK, Virkkula A, Hillamo R, Kerminen V-M andKulmalaM. Number
14 size distributions of marine aerosols: observations during a cruise between
15 the EnglishChannel and coast of Antarctica *J. Geophys. Res.* 107 4753, 2002
16
- 17 Koponen IK, Virkkula A, Hillamo R, Kerminen V-M andKulmalaM Number size
18 distributions and concentrations of the continental summer aerosols in Queen
19 Maud Land, Antarctica *J. Geophys. Res.* 108 4587, 2003
20
- 21 Korhonen, H., Carslaw, K. S., Spracklen, D. V., Mann, G., W., and Woodhouse,
22 M. T.: Influence of oceanic dimethyl sulfide emissions on cloud condensation
23 nuclei concentrations and seasonality over the remote Southern Hemisphere
24 oceans: A global model study, *J. Geophys. Res.-Atmos.*, 113, D15204,
25 [doi:10.1029/2007JD009718](https://doi.org/10.1029/2007JD009718), 2008
26
- 27 Laaksonen, A., Kulmala, M., O'Dowd, C. D., Joutsensaari, J., Vaattovaara, P.,
28 Mikkonen, S., Lehtinen, K. E. J., Sogacheva, L., DalMaso, M., Aalto, P.,
29 Petäjä, T., Sogachev, A., Yoon, Y. J., Lihavainen, H., Nilsson, D., Facchini, M.
30 C., Cavalli, F., Fuzzi, S., Hoffmann, T., Arnold, F., Hanke, M., Sellegri, K.,
31 Umann, B., Junkermann, W., Coe, H., Allan, J. D., Alfarra, M. R., Worsnop,
32 D. R., Riekkola, M. -L., Hyötyläinen, T., and Viisanen, Y.: The role of VOC
33 oxidation products in continental new particle formation, *Atmos. Chem. Phys.*,
34 8, 2657–2665, [doi:10.5194/acp-8-2657-2008](https://doi.org/10.5194/acp-8-2657-2008), 2009
35
- 36 Lange, R., Dall'Osto, M., Skov, H., Nielsen, I. E., David Beddows, Simo, R.,
37 Roy Harrison & Massling, A., 29 Mar 2018, Characterization of distinct Arctic
38 Aerosol Accumulation Modes and their Sources, *Atmospheric Environment*.
39 183, p. 1-10
40
- 41 Liu, J., Dedrick, J., Russell, L. M., Senum, G. I., Uin, J., Kuang, C., Springston,
42 S. R., Leaitch, W. R., Aiken, A. C., and Lubin, D.: High summertime aerosol
43 organic functional group concentrations from marine and seabird sources at
44 Ross Island, Antarctica, during AWARE, *Atmos. Chem. Phys.*, 18, 8571–8587,
45 <https://doi.org/10.5194/acp-18-8571-2018>, 2018.
46
- 47 McCoy, D. T., Burrows, S. M., Wood, R., Grosvenor, D. P., Elliott, S. M., Ma,
48 P.-L., Rasch, P. J., and Hartmann, D.L.: Natural aerosols explain seasonal
49 and spatial patterns of Southern Ocean cloud albedo, *Sci. Adv.*, 1, e1500157,
50 <https://doi.org/10.1126/sciadv.1500157>, 2015

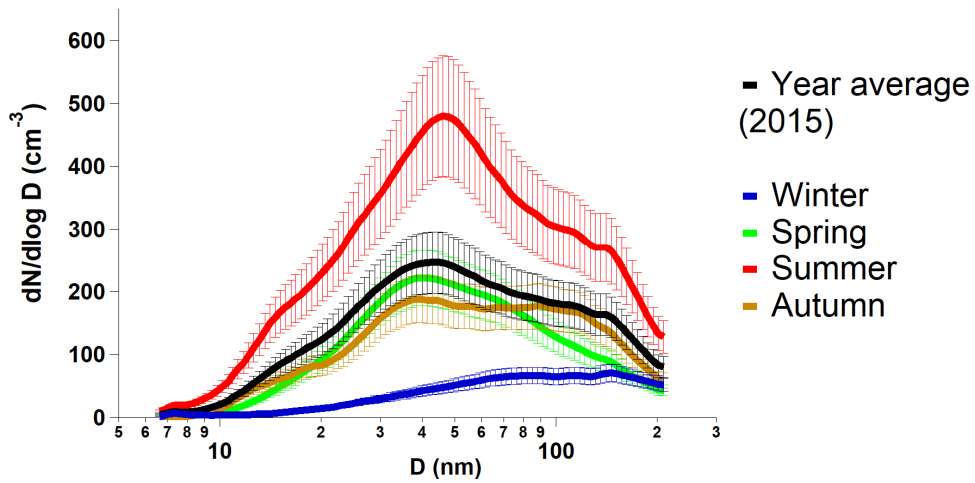
1
2 Murphy, D. M., Froyd, K. D., Bian, H., Brock, C. A., Dibb, J. E., DiGangi, J.
3 P., Diskin, G., Dollner, M., Kupc, A., Scheuer, E. M., Schill, G. P., Weinzierl, B.,
4 Williamson, C. J., and Yu, P.: The distribution of sea-salt aerosol in the global
5 troposphere, *Atmos. Chem. Phys.*, 19, 4093-4104,
6 <https://doi.org/10.5194/acp-19-4093-2019>, 2019.
7
8 O'Dowd, C.D., Smith, M.H., Consterdine, I.E., Lowe, J.A., 1997a. Marine
9 aerosol, sea-salt, and the marinesulphur cycle—a short review. *Atmos. Environ.*
10 31, 73–80, 1997a
11
12 O'Dowd, CO, J. A. Lowe, M. H. Smith, B. Davison, C. N. Hewitt, R. M.
13 Harrison, Biogenic sulphur emissions and inferred non-sea-salt-sulphate cloud
14 condensation nuclei in and around Antarctica. *J. Geophys. Res. Atmos.* 102,
15 12839–12854, 1997b
16
17 Quinn, P. K. and Bates, T. S.: The case against climate regulation via oceanic
18 phytoplankton sulphur emissions, *Nature*,480(7375), 51–56,
19 [doi:10.1038/nature10580](https://doi.org/10.1038/nature10580), 2011
20
21 Quinn, P. K., Collins, D. B., Grassian, V. H., Prather, K. A.,and Bates, T. S.:
22 Chemistry and Related Properties of Freshly Emitted Sea Spray Aerosol, *hem.*
23 *Rev.*, 115, 4383–4399, [doi:10.1021/cr500713g](https://doi.org/10.1021/cr500713g), 2015
24
25 Quinn, P. K., Coffman, D. J., Johnson, J. E., Upchurch, L. M., and Bates, T. S.:
26 Small fraction of marine cloud condensation nuclei made up of sea spray
27 aerosol, *Nat. Geosci.*, 10, 674–679, <https://doi.org/10.1038/ngeo3003>, 2017.
28
29 Rankin, A. M., and E. W. Wolff, A year-long record of size-segregated aerosol
30 composition at Halley, Antarctica, *J. Geophys. Res.*, 108(D24), 4775,
31 [doi:10.1029/2003JD003993](https://doi.org/10.1029/2003JD003993), 2003.
32
33 Reddington, C., Carslaw, K., Stier, P., Schutgens, N., Coe, H., Liu, D., Allan, J.,
34 Pringle, K., Lee, L., and Yoshioka, M.: The Global Aerosol Synthesis and
35 Science Project (GASSP): measurements and modelling to reduce uncertainty,
36 *B. Am. Meteorol. Soc.*, 98.9, 1857–1877, 2017.
37
38 Richard A. Becker, Allan R. Wilks. R version by Ray Brownrigg.
39 Enhancements by Thomas P Minka and Alex Deckmyn. (2018). maps: Draw
40 Geographical Maps. R package version 3.3.0. [https://CRAN.R-](https://CRAN.R-project.org/package=maps)
41 [project.org/package=maps](https://CRAN.R-project.org/package=maps)
42
43 Robert J. Hijmans (2019). raster: Geographic Data Analysis and Modeling. R
44 package version 2.9-23. <https://CRAN.R-project.org/package=raster>
45
46 Roscoe, H. K., A. E. Jones, N. Brough, R. Weller, A. Saiz-Lopez, A. S.
47 Mahajan, A. Schoenhardt, J. P. Burrows, and Z. L. Fleming (2015), Particles
48 and iodine compounds in coastal Antarctica, *J. Geophys. Res. Atmos.*, 120,
49 7144–7156, [doi:10.1002/2015JD023301](https://doi.org/10.1002/2015JD023301).
50

- 1 Rousseeuw, P.,J., (1987) Silhouettes: a graphical aid to the interpretation and
2 validation of cluster analysis, *Journal of Computational and Applied*
3 *Mathematics* 20, 53-65.
4
5
- 6 Saiz-Lopez, A., A. S. Mahajan, R. A. Salmon, S. J.-B. Bauguitte, A. E. Jones,
7 H. K. Roscoe, and J. M. C. Plane (2007), *Boundary layer halogens in coastal*
8 *Antarctica*, *Science*, 317, 348–351.
9
- 10 Sanchez, K. J., Chen, C.-L., Russell, L. M., Betha, R., Liu, J., Price, D. J.,
11 Massoli, P., Ziemba, L. D., Crosbie, E. C., Moore, R. H., Müller, M., Schiller, S.
12 A., Wisthaler, A., Lee, A. K. Y., Quinn, P. K., Bates, T. S., Porter, J., Bell, T.
13 G., Saltzman, E. S., Vaillancourt, R. D., and Behrenfeld, M. J.: Substantial
14 seasonal contribution of observed biogenic sulfate particles to cloud
15 condensation nuclei, *Sci. Rep.*, 8, 3235, [https://doi.org/10.1038/s41598-](https://doi.org/10.1038/s41598-018-21590-9)
16 [018-21590-9](https://doi.org/10.1038/s41598-018-21590-9), 2018.
17
- 18 Schmale, J., Schneider, J., Nemitz, E., Tang, Y. S., Dragosits, U., Blackall, T.
19 D., Trathan, P. N., Phillips, G. J., Sutton, M., and Braban, C. F.: Sub-Antarctic
20 marine aerosol: dominant contributions from biogenic sources, *Atmos. Chem.*
21 *Phys.*, 13, 8669– 8694, <https://doi.org/10.5194/acp-13-8669-2013>, 2013.
22
- 23 Schönhardt, A., A. Richter, F. Wittrock, H. Kirk, H. Oetjen, H. K. Roscoe, and
24 J. P. Burrows (2008), Observations of iodine monoxide (IO) columns from
25 satellite, *Atmos. Chem. Phys.*, 8, 637–653 Shaw G.E. 1988 Antarctic
26 aerosols: a review *Rev. Geophys.* 26 89–112
27
- 28 Sipilä, M., Sarnela, N., Jokinen, T., Henschel, H., Junninen, H., Kontkanen, J.,
29 Ichners, S., Kangasluoma, J., Franchin, A., 5 Peräkylä, O., Rissanen, M.P., hn,
30 M., Vehkamäki, H., Kurten, T., Berndt, T., Petäjä, T., Worsnop, D., Ceburnis, .,
31 Kerminen, V.-M., Kulmala, M., O'Dowd, C., 2016. Molecular-scale evidence of
32 aerosol particle formation via sequential addition of HIO₃. *Nature* 537, 532–
33 534. <https://doi.org/10.1038/nature19314>.
34
- 35 Shaw, G. E.: Considerations on the Origin and Properties of the Antarctic
36 Aerosol, *Rev. Geophys.*, 17, 1983–1998, 1988.
37
- 38 Teinilä, K., Frey, A., Hillamo, R., Tülp, H. C., and Weller, R.: A study of the
39 sea-salt chemistry using size-segregated aerosol measurements at coastal
40 Antarctic station Neumayer, *Atmos. Environ.*, 96, 11–19, 2014.
41
- 42 Udisti, R., Dayan, U., Becagli, S., Busetto, M., Frosini, D., Legrand, M.,
43 Lucarelli, F., Preunkert, S., Severi, M., Traversi, R., and Vitale, V.: Sea spray
44 aerosol in central Antarctica. Present atmospheric behaviour and implications
45 for paleoclimatic reconstructions, *Atmos. Environ.*, 52, 109–
46 120, <https://doi.org/10.1016/j.atmosenv.2011.10.018>, 2012.
47
- 48 Vallina, S. M. and Simó, R.: Re-visiting the CLAW hypothesis, *Environ. Chem.*,
49 4, 384–387, <https://doi.org/10.1071/EN07055>, 2007.
50

1 Vignon, É., Traullé, O., and Berne, A.: On the fine vertical structure of the low
2 troposphere over the coastal margins of East Antarctica, *Atmos. Chem. Phys.*,
3 19, 4659–4683, <https://doi.org/10.5194/acp-19-4659-2019>, 2019.
4
5 Virkkula, A., Teinilä, K., Hillamo, R., Kerminen, V.-M., Saarikoski, S., Aurela,
6 M., Viidanoja, J., Paatero, J., Koponen, I. K., Kulmala, M.: Chemical
7 composition of boundary layer aerosol over the Atlantic Ocean and at an
8 Antarctic site, *Atmos. Chem. Phys.*, 6, 3407–3421, 2006.
9
10 Yang, X., Frey, M. M., Rhodes, R. H., Norris, S. J., Brooks, I. M., Anderson, P.
11 S., Nishimura, K., Jones, A. E., and Wolff, E. W.: Sea salt aerosol production
12 via sublimating wind-blown saline snow particles over sea ice:
13 parameterizations and relevant microphysical mechanisms, *Atmos. Chem.*
14 *Phys.*, 19, 8407–8424, <https://doi.org/10.5194/acp-19-8407-2019>, 2019.
15
16 Weller, R., Minikin, A., Wagenbach, D., and Dreiling, V.: Characterization of
17 the inter-annual, seasonal, and diurnal variations of condensation particle
18 concentrations at Neumayer, Antarctica, *Atmos. Chem. Phys.*, 11, 13243–
19 13257, <https://doi.org/10.5194/acp-11-13243-2011>, 2011.
20
21 Weller, R., Schmidt, K., Teinilä, K., and Hillamo, R.: Natural new particle
22 formation at the coastal Antarctic site Neumayer, *Atmos. Chem. Phys.*, 15,
23 11399–11410, <https://doi.org/10.5194/acp-15-11399-2015>, 2015.
24
25 Weller, R., Legrand, M., and Preunkert, S.: Size distribution and ionic
26 composition of marine summer aerosol at the continental Antarctic site
27 Kohnen, *Atmos. Chem. Phys.*, 18, 2413–2430, [https://doi.org/10.5194/acp-18-](https://doi.org/10.5194/acp-18-2413-2018)
28 [2413-2018](https://doi.org/10.5194/acp-18-2413-2018), 2018.
29
30 Xu, G. J., Gao, Y., Lin, Q., Li, W., and Chen, L. Q.: Characteristics of water-
31 soluble inorganic and organic ions in aerosols over the Southern Ocean and
32 coastal East Antarctica during austral summer, *J. Geophys. Res.-Atmos.*, 118,
33 13303–13318, <https://doi.org/10.1002/2013jd019496>, 2013.
34
35 Zorn, S. R., Drewnick, F., Schott, M., Hoffmann, T., and Borrmann, S.:
36 characterization of the South Atlantic marine boundary layer aerosol using an
37 aerodyne aerosol mass spectrometer, *Atmos. Chem. Phys.*, 8, 4711–4728,
38 <https://doi.org/10.5194/acp-8-4711-2008>, 2008.
39
40
41
42
43
44
45
46
47

1
2
3
4
5
6
7
8
9
10
11
12
13
14
15
16
17
18

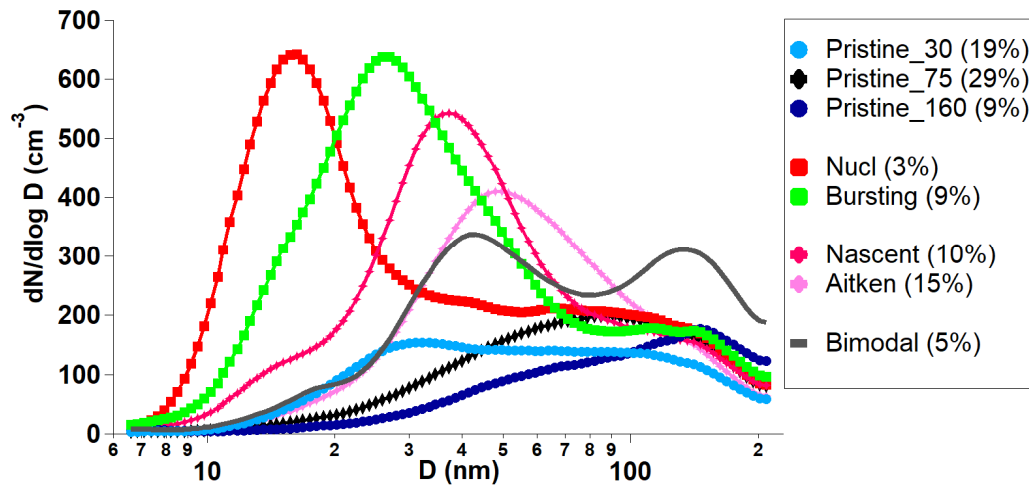
LIST OF FIGURES



19
20
21
22
23
24

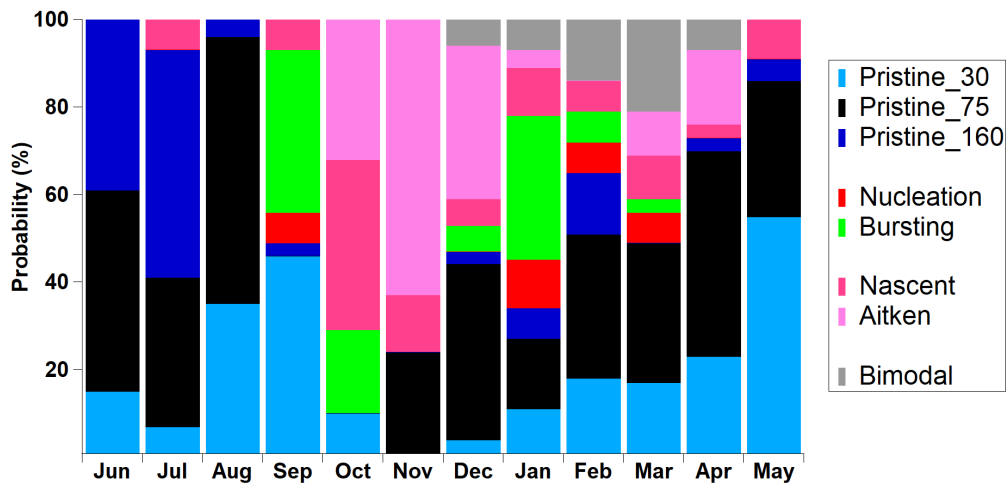
Figure 1 Seasonal mean aerosol size distribution measured by the SMPS at Halley VI research station over the year 2015. The error bars represent the standard deviation of the measurements from the mean value.

1
2
3
4
5
6
7
8
9
10
11
12



(a)

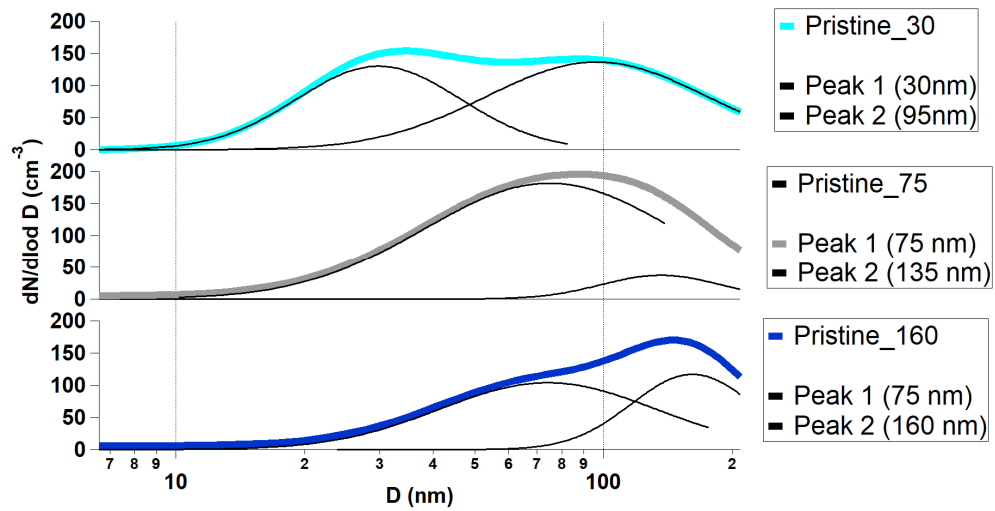
13
14
15
16



(b)

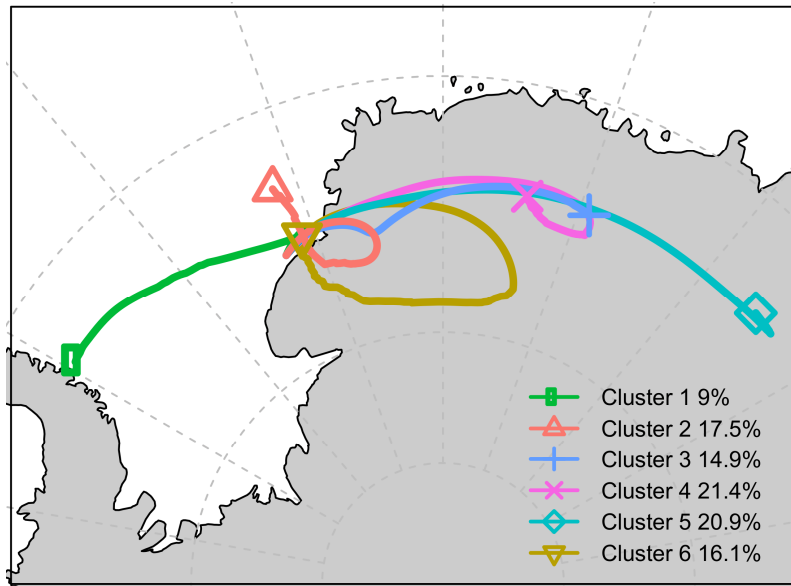
Figure 2 (a) Size distributions of the 8 k-means clusters and (b) annual frequency distributions of the six aerosol categories

1
2
3
4
5
6
7
8
9
10
11
12
13
14
15
16
17



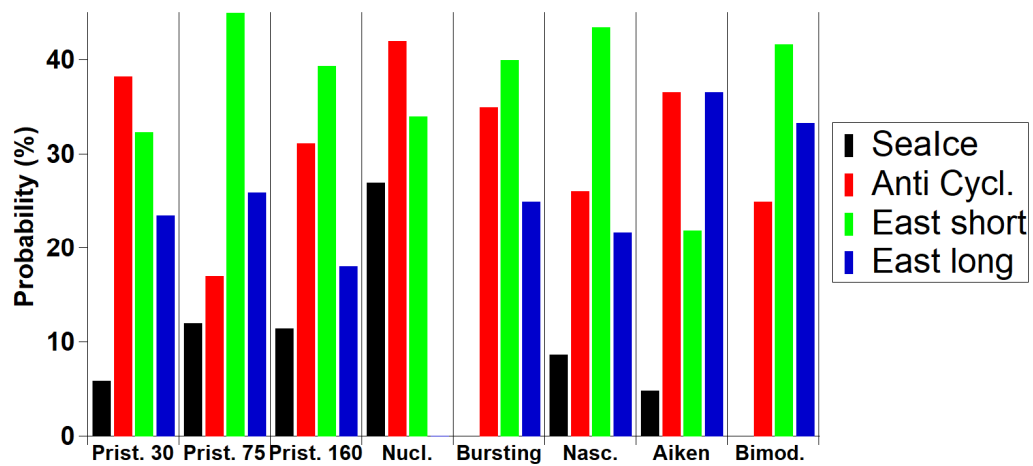
1
2
3
4
5
6
7
8
9
10
11
12
13
14
15
16
17
18
19

Figure 3 Peak fitting of the 3 pristine K-means aerosol categories.



1
2

(a)

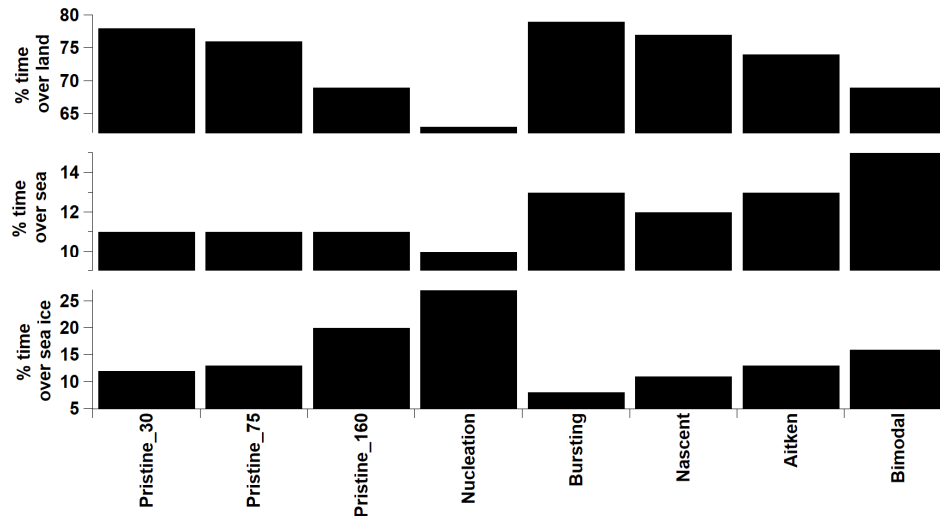


3
4

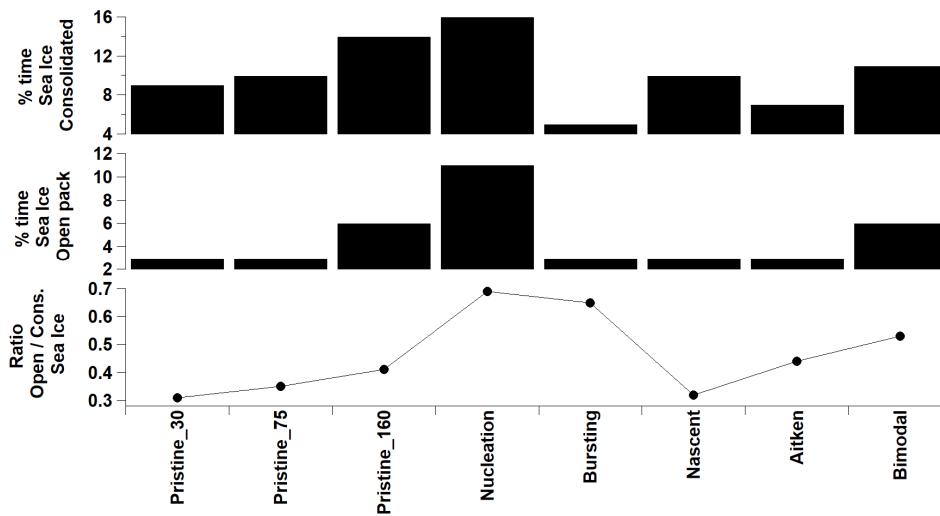
(b)

5 **Figure 4 (a)** Air mass analysis of air mass back trajectories arriving at Halley
 6 during the year 2015 (hourly resolution) and **(b)** relative contribution for each
 7 aerosol category. Groups in (b) are : Sea Ice (1), Anti Cycl. (2,6), East short
 8 (3,4) and east long (5),

9
10
11



(a)



(b)

Figure 5 (a) Percentages of air masses over land, sea, and sea ice for the 8 K-means aerosol categories and (b) percentages of consolidated and open pack sea ice, and open pack / consolidated ratio.

1
2
3
4
5
6
7
8
9
10
11
12
13
14
15
16
17
18
19
20
21
22
23
24
25

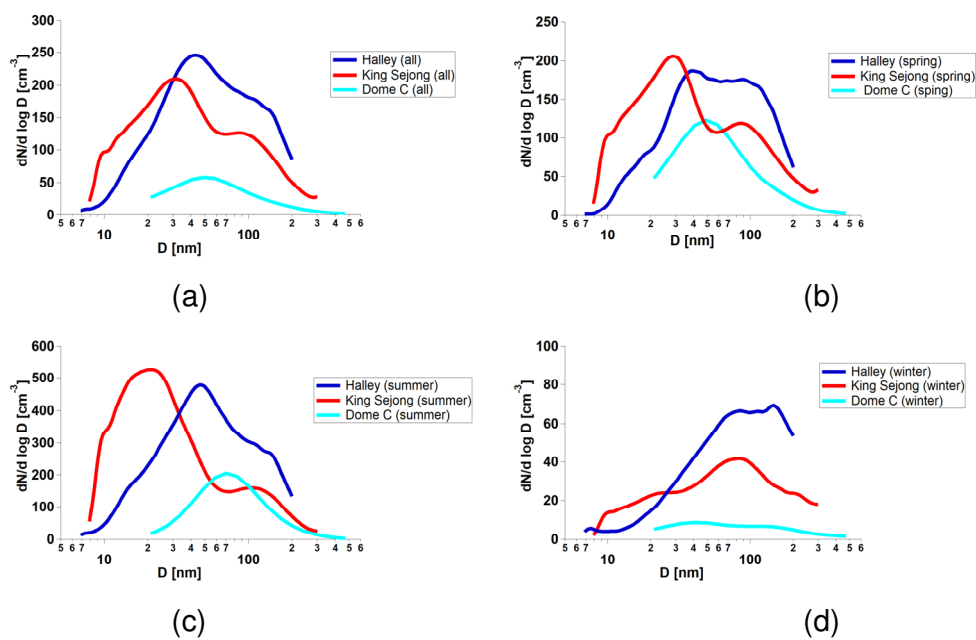
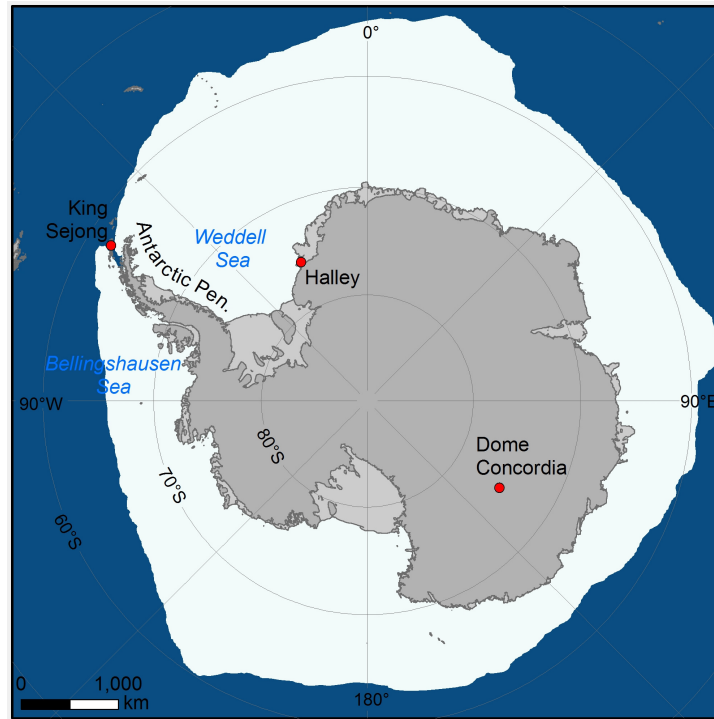


Figure 6. Average size-resolved particle size distributions simultaneously measured during the year 2015 at Halley, Dome C and King Sejong stations for (a) May-December (8 months), (b) spring (Sep., Oct., Nov., 3 months), (c) summer (December, 1 month) and (d) winter (Jun., Jul., Aug., 3 months).

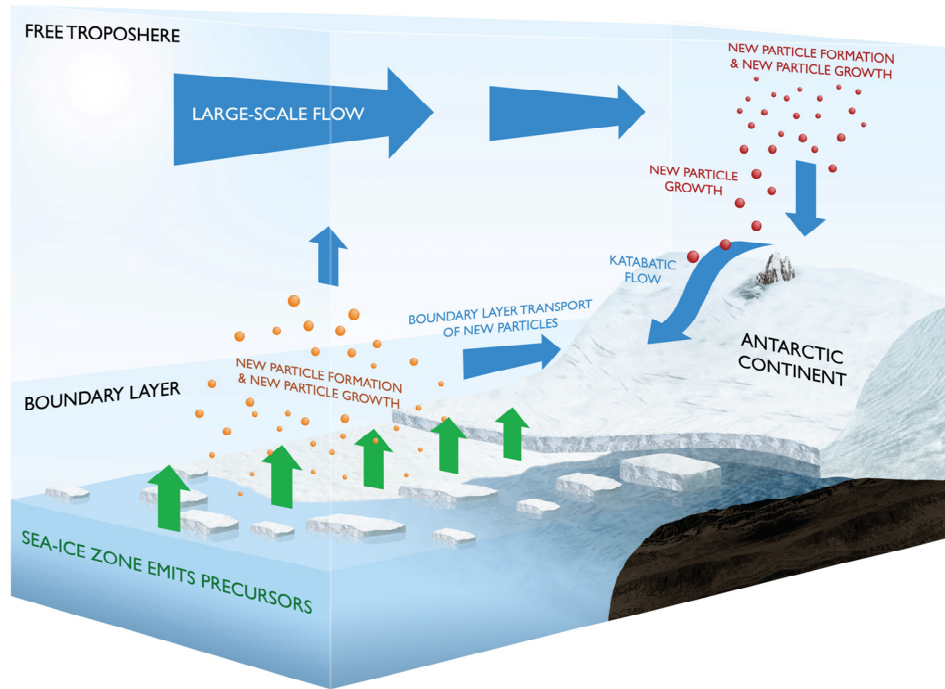
1
2



3
4
5
6
7
8
9
10
11
12
13
14
15
16
17
18
19
20

Figure 7. Map with locations of Antarctic monitoring stations considered in Figure 6. Please note that the sea ice extent is the median September extent from 1981-2010 (data are from NSIDC - <https://nsidc.org/data/g02135>).

1



2

3

4 **Figure 8** Schematic illustrations of the ultrafine New Particle Formation (NPF)

5 and New Particle Growth (NPG) aerosols in Antarctica.

6

7

8

9

10

11

12

13

14

15

16

17

18